JGR Biogeosciences

RESEARCH ARTICLE
10.1029/2023JG007588

Similarities in Storage and Transport of Sulfate in Forested and Suburban Watersheds, Despite Anthropogenically Elevated Suburban Sulfate

C. L. Cosans[1], **M. L. Gomes**[2], **M. J. Marsh**[3], **J. Moore**[3], and **C. J. Harman**[1]

[1]Environmental Health and Engineering, Johns Hopkins University, Baltimore, MD, USA, [2]Department of Earth and Planetary Sciences, Johns Hopkins University, Baltimore, MD, USA, [3]Department of Physics, Astronomy, and Geosciences, Towson University, Towson, MD, USA

Key Points:

- The suburban stream has elevated sulfate concentrations and fluxes, likely due to contributions from septic systems and lawn care
- Sulfate mobilized in seasonal- and event-scale wet conditions in both forested and suburban streams
- Sulfate in the suburban stream is associated with soil storage mobilized in wet conditions, not runoff from impervious surfaces

Supporting Information:

Supporting Information may be found in the online version of this article.

Correspondence to:

M. L. Gomes,
mgomes@jhu.edu

Citation:

Cosans, C. L., Gomes, M. L., Marsh, M. J., Moore, J., & Harman, C. J. (2024). Similarities in storage and transport of sulfate in forested and suburban watersheds, despite anthropogenically elevated suburban sulfate. *Journal of Geophysical Research: Biogeosciences*, *129*, e2023JG007588. https://doi.org/10.1029/2023JG007588

Received 22 MAY 2023
Accepted 7 DEC 2023

Abstract

Sulfate is a potential pollutant and important nutrient linked with the nitrogen, carbon, and phosphorus cycles. The importance of different anthropogenic sulfate sources in suburban streams (septic systems, fertilizer, road salt, and infrastructure) is uncertain, and the temporal dynamics of stream export sparsely documented. We study sources and export dynamics of sulfate in suburban and forested headwater catchments. Stream baseflow discharge and sulfate concentrations were strongly positively correlated in both watersheds with the highest values in spring. Suburban concentrations and fluxes (2.48–7.5 mg/L or 25.8–78.1 µM, 16.6 kg/ha/yr) were consistently higher than forested (0.56–2.78 mg/L or 5.8–28.9 µM, 5 kg/ha/yr). Following precipitation, sulfate concentrations in both forested and suburban streams increased to concentrations above pre-storm values and remained high after peak discharge. These dynamics suggest that both catchments have a large pool of sulfate that can be mobilized under wet conditions. Ridge-top forest soil samples contained 210 kg/ha stored, extractable sulfate. Current atmospheric sulfate deposition rates (5–7 kg/ha/yr) are approximately in balance with sulfate export in the forested stream. In the suburban watershed, we estimated septic fields contribute up to 11 kg/ha/yr (about half from surfactants) and lawn care up to 4.3 kg/ha/yr and are the most likely sources of elevated stream sulfate. Sulfate sulfur (4.9–5.8‰ forested; 6.1–7.0‰ suburban) and oxygen isotope values (0.7–2.0‰ forested; −0.1–4.1‰ suburban) are consistent with this interpretation, but do not provide strong corroboration due to large variation and overlap in estimated source values.

Plain Language Summary

Sulfate can be a nutrient or pollutant that alters stream biogeochemistry depending on dissolved concentrations. For decades, atmospheric sulfur deposition was elevated due to regional anthropogenic emissions. Regulation in the 1990s resulted in decreasing deposition and increasing importance of other sulfur sources, for example, associated with land use. We studied suburban sulfate sources, including infrastructure and activities not widely recognized as sources of stream sulfate. We measured dissolved sulfate concentrations and sulfate tracer isotopes in neighboring forested and suburban watersheds. Sulfate inputs and exports are compared with budgets of possible sulfate contributions to the stream from septic systems, lawn care, road salt, building materials, and historic agriculture. The suburban stream exports about 3x more sulfate a year from the watershed than the forested stream. Extra suburban stream sulfate appears to be largely caused by human waste and cleaning products flowing to septic fields and lawn care. More sulfate is transported to the stream during the wetter spring and after rain. This elevated transport may be because the groundwater table moves upwards during wetter times and transports sulfate that was stored in soil to the stream. Identifying suburban sources of sulfate pollution is important to protecting stream health.

1. Introduction

Sulfate is an essential nutrient that undergoes complex biogeochemical cycling and is linked to the carbon, nitrogen, and phosphorus cycles (Caraco, 1993; Hao et al., 2014; Reverey et al., 2016; Zhu et al., 2018). It also can acts as a pollutant with potentially important ecological consequences (Burke et al., 2018; Cook et al., 2000; Evans et al., 1997; Lamers et al., 1998; Pester et al., 2012). Sulfate has been extensively studied in the context of its role in acid rain, with atmospheric sulfate produced by fossil fuel combustion impacting ecosystems and degrading infrastructure (Charola et al., 2007; Likens & Bormann, 1974). Acidity generated by the release of sulfate or oxidation of metal sulfide can also impact rates of chemical weathering in the landscape (Johnson et al., 1981), and contributes to transient atmospheric carbon dioxide rise on geological timescales (Calmels et al., 2007; Torres et al., 2016). In addition to impacts of acidification, sulfate can promote the mobilization of phosphate into surface waters because sulfide produced from the microbially mediated reduction of sulfate competes for adsorption sites to iron minerals in sediments (Caraco et al., 1993; Roden & Edmonds, 1997). In some systems, sulfate reduction and subsequent oxidation of the produced sulfide promotes nitrogen loss through denitrification and anaerobic oxidation of ammonia (Canfield et al., 2010; Cardoso et al., 2006). Understanding sulfur sources and transport are essential for understanding biogeochemical cycles and mitigating nutrient ecological impacts.

Elevated sulfate concentrations (relative to streams in forested catchments) have been observed in streams with suburban or urban land cover (Cravotta, 1995; Kaushal & Belt, 2012; Kaushal et al., 2017; Lewis et al., 2007; Moore et al., 2017) and in some cases agricultural land use (Caraco, 1993; Hinckley et al., 2020; Taboada-Castro et al., 2015). However, research on sulfate in surface waters has mostly focused on atmospheric deposition and has been predominantly based on data from forested catchments (Christophersen & Wright, 1981; Johnson et al., 1981; Likens & Bormann, 1974; Lindberg et al., 1986). Those research efforts contributed to justification for the highly successful Clean Air Amendment in 1990, which has resulted in large declines in atmospheric deposition nationally and stream sulfate concentrations in some regions (Eng & Scanlon, 2021; Gislason & Torssander, 2006; Lawrence, 2002; Rice et al., 2014; Riscassi et al., 2019). Despite large scale reductions in atmospheric emissions, concern is growing that other anthropogenic sulfur sources are increasing and may reduce gains made by the Clean Air Act (Hinckley et al., 2020). These additional, potentially substantial, land use related sources include fertilizer, pesticides, soil amendment products, building materials such as concrete and brick, road salt, and sewage.

Additional sources that may be important in (sub)urban settings include road salt, infrastructure materials, fertilizer, soil conditioners, and sewage. Road salt and weathering of concrete infrastructure have both been proposed as anthropogenic stream sulfate sources in urban contexts (Bird et al., 2018; Blaszczak et al., 2019; Kaushal et al., 2017; Moore et al., 2017). Strong correlation of sulfate and chloride concentrations in synoptic baseflow data from an urban watershed in the Baltimore region suggests that these two constituents are entering groundwater at similar locations; sulfate and chloride concentrations showed strong positive spatial correlation with groundwater flow paths originating from areas with high impervious surface cover (located 250–2,500 m from the stream) and weaker but positive correlation with sewer pipes close to the stream and urban fill farther from the stream (Welty et al., 2023). Sulfate sources remained somewhat unclear with urban fill that includes construction materials proposed as a substantial contributor; by contrast, chloride was predominantly from deicing salt (Welty et al., 2023). Suburban lawn fertilizer use may be widespread (Fraser et al., 2013) and sulfur may be applied to alkaline lawn and garden soils as a conditioner to manage pH (Shober et al., 2011). Septic fields, leaky sewer pipes, and treated wastewater effluent also have been linked to elevated sulfate in streams (Blaszczak et al., 2019; Lewis et al., 2007; Wilhelm, Schiff, & Robertson, 1994). Identifying suburban sulfate sources and characterizing the fluxes of sulfate from different sources to surface waters is essential to assessing the biogeochemical effects of sulfate in (sub)urban systems.

We investigate which suburban sources contribute substantial sulfate to surface waters and how suburban land use impacts sulfate storage in the landscape and mobilization. This study focuses on neighboring forested and suburban headwater catchments in the Maryland Piedmont, both of which are in the highly nutrient-impacted Chesapeake Bay watershed (S. B. Bricker et al., 2008). The catchments are nested within a 381 ha mixed land use catchment and have similar geology and legacies of atmospheric inputs. Thus, these two catchments serve as useful locations to consider the impacts of suburban development on stream sulfate fluxes. Below we (a) investigate stream sulfate concentrations and fluxes across seasonal and storm event timescales to understand sulfate mobilization and transport, (b) develop sulfate flux budgets for the catchments to determine the magnitude and relevance of different potential anthropogenic sulfate sources, and (c) compare sulfate sulfur and oxygen isotope compositions in stream water and sources across land uses to make inferences about water source mixing and mobilization during storm events.

2. Methods

2.1. Study Location

The study area is in the eastern United States and is comprised of small, headwater catchments nested in the larger Baisman Run catchment in Cockeysville, MD, 12 km north of Baltimore, MD (Figure 1, Table 1).

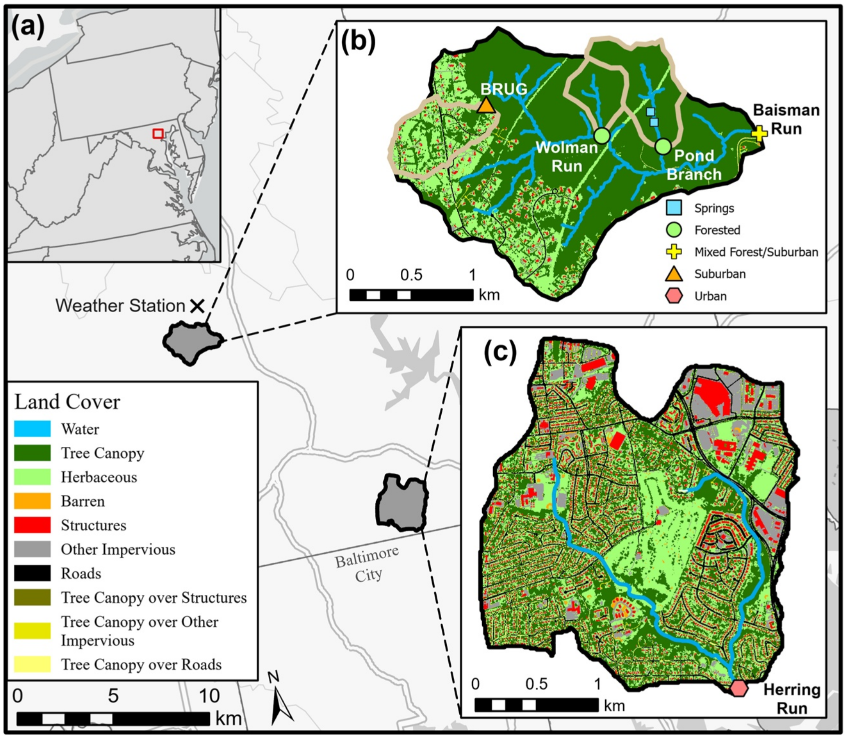

Figure 1. (a) Location map of the study catchments and regional reference catchment within the Mid-Atlantic U.S. and Baltimore metropolitan area, Maryland. (b) Detail map of the larger, mixed land use Baisman Run catchment (yellow cross) and the smaller, nested suburban Baisman Run Upper Gage catchment (orange triangle) and forested Wolman Run and Pond Branch catchments (green circles). Spring sampling locations are denoted with blue squares. (c) Detail map of West Branch of Herring Run, the regional urban reference catchment (red hexagon). Detail maps show land use and stream networks based on the 2017/2018 Chesapeake Conservancy Land Cover Dataset (Chesapeake Bay Program Office, 2022) and 2017 (U.S. Geological Survey, 2017) NHD Plus, respectively.

Baisman Run is located in the deeply weathered Piedmont Province, and is entirely underlain by the Loch Raven Schist (Crowley et al., 1975). The Baisman Run catchment has mixed land cover containing forested (Pond Branch [PB] and Wolman Run) and low-density suburban (Baisman Run Upper Gage [BRUG] headwater sub catchments (Figure 1, Table 1). Residents in the suburban BRUG catchment have septic systems and are not connected to a centralized sanitary sewer system. The nearby forested and suburban headwater catchments offer a useful case study for comparing sulfate fluxes across land use, with both sites having similar size, geology, and atmospheric inputs. Two natural springs at the toes of hillslopes in the forested PB catchment were dug out during previous research to facilitate sample collection (Figure 1, Putnam, 2018). Pond Branch has been a field site for several geochemical, geophysical, and hydrological research projects (Band et al., 2001; Bird et al., 2018; O. P. Bricker et al., 1968; Castiblanco et al., 2023; Clair et al., 2015; Cleaves et al., 1970; Duncan et al., 2017; Groffman et al., 2004; McMahon et al., 2021; Moore et al., 2017; Wolman, 1987). A weather

Table 1
Summary of the Study Catchments Including Land Use, Stream Gage Identifiers, and Drainage Area for the Catchments

Catchment	Land use	Gage	Area (ha)	Location
Baisman Run	Mixed suburban and forest	USGS 01583580	381	39°28′46″N, 76°40'41″W
Baisman Run Upper Gage	Suburban	JHU (Putnam, 2018)	35	39°29′08″N, 76°42′10″W
Pond Branch	Forest	USGS 01583570	37	39°28′49″N, 76°41′15″W
Wolman Run	Forest	None	18	39°28′53″N, 76°41′33″W
West Branch Herring Run	Urban	USGS 01585219	260	39°22′25″N, 76°35′04″W

Note. Baisman Run Upper Gage (BRUG), Pond Branch, and Wolman Run are nested in the larger Baisman Run catchment.

station is located approximately half a mile north of the catchment and includes a tipping bucket to measure precipitation rates and a mounted funnel and bottle precipitation collector (Figure 1). BRUG also has been previously studied, with prior work at this field site establishing a temporary 45°, 8 inch deep v-notch weir for continuously gaged discharge of BRUG in the flume previously used to study sediment loads (Putnam, 2018; Wolman, 1987). The West Branch of Herring Run, located about 18 km away, provides a regional urban catchment reference (Table 1) and is underlain by Baltimore Gneiss, which has similar chemistry to the Loch Raven Schist.

2.2. Discharge Measurement and Modeling

Discharge data were a combination of USGS data (PB and Baisman Run; U. S. Geological Survey, 2016) and data collected for this study (BRUG). The USGS discharge data (15-min interval) extend across the whole period while the data for BRUG were collected from September 2017 to December 2018. The BRUG weir and flume water level data were monitored using Solinst levelogger pressure transducers compensated for atmospheric pressure using a Solinst barologger. The water level was converted to discharge using the v-notch weir equation (Dingman, 2015). The rectangular flume equation was used to correct rare instances where the v-notch was overtopped (Dingman, 2015). We used the relationship between the BRUG discharge and the USGS PB and Baisman Run gages to extend the BRUG discharge (Q) over the entire period of record. BRUG, PB, and Baisman Run discharge were separated into baseflow and quick flow using a recursive digital filter (BFI = 0.99, a = 0.9999) using the method of Eckhardt (2005) and then smoothed to a 6 hr interval. The recursive digital filter is a two-parameter filter that models the volume of discharge that is baseflow by smoothing rapid changes in the total discharge during periods where stream discharge is impacted by storm events (Eckhardt, 2005). The baseflow separation was performed for periods of stream discharge from 3 hr before the start of a precipitation event to 12 hr after the end of detection of precipitation at the weather station. Stream discharge during all other time periods was classified as entirely baseflow. Separated discharge data were normalized using a maximum-likelihood Box-Cox transformation. BRUG baseflow and peak flow were then modeled separately through linear regression (baseflow $r^2 = 0.91$, quick flow $r^2 = 0.74$).

2.3. Sample Collection

Water samples were collected at multiple locations and timescales for sulfate concentration analysis. Weekly grab samples at the gages for PB, BRUG, Wolman Run, both forest springs, and weekly aggregated precipitation samples from the weather station were collected from April 2015 to April 2017. Higher resolution storm sampling (15 min–2 hr) was performed in May 2018 for BRUG and PB using Teledyne ISCO™ portable samplers. A bulk precipitation sample was also collected over the course of the May 2018 storm at the weather station. Samples were filtered through 0.45-micron polypropylene filters upon collection and refrigerated until analysis. Storm sampling included samples for stable water isotope analysis which were stored in parafilmed, glass polyseal vials to prevent isotope fractionation associated with evaporation. Stable water isotope samples also were collected from the ISCO autosampler within 24 hr. The weekly sampling period is used for estimating annual catchment sulfate budgets, which change gradually on the decadal scale in the southern Piedmont (Eng & Scanlon, 2021). Since storm data do not overlap with the weekly sample collection period, the storm data are considered separately and offer additional information about concentration dynamics across changes in streamflow at a shorter timescale.

Stream and source candidate samples were collected to investigate sulfate sulfur and oxygen isotope compositions as sulfate source tracers. From March 2019 to February 2020 approximately monthly, larger volume samples of 4, 6, and 14 liters were collected for Herring Run, BRUG, and PB, respectively, to obtain sufficient sulfate for isotope analysis. Storm targeted large volume samples were also collected in May 2018 and April and November 2019. Twenty-five mL of 3% zinc acetate was added per liter of sample for the sulfate isotope samples upon collection to stop biological activity and fix any sulfides as zinc sulfide. Grab samples of possible anthropogenic sulfate sources were collected from the suburban and urban areas including asphalt, concrete, road salt, and soil acidifier garden product. Soil samples were augured from the PB ridge down to 160 cm and small amounts of iron sulfides were sampled with a dental drill from a bedrock core at 19, 24, and 32 m below the ridge. Additional sulfate source isotope values published in literature for atmospheric deposition, fertilizer, and septic effluent, were also considered.

2.4. Sample Analysis

All water samples were analyzed for sulfate concentrations and stable water isotope ratios. Sulfate concentrations were determined on a Dionex ICS-5000 ion chromatograph (IC). The lowest standard used for calibration on the IC is 0.37 ppm and lower concentrations are measurable, however a conservative detection limit for accurate measurement of concentration is 0.5 ppm. Check standards were run every 15–20 samples, and samples were rerun if standards were >10% different from the expected value. The precipitation and 15 min storm samples were analyzed for oxygen and hydrogen isotope compositions using a Los Gatos Research Liquid Water Isotope Analyzer Off-Axis Integrated Cavity Output Spectroscopy system. Data post processing was performed using the LGR LWIA post analysis software version 2.1 with USGS standards 46, 47, and 48. The isotope compositions are reported in permil (‰) units using delta notation ($\delta^{18}O_{H_2O}$, δ^2H) with the relationship: $\delta_x = \left(\frac{R_{sample} - R_{standard}}{R_{standard}}\right)$ where R is the $^{18}O/^{16}O$ or $^2H/^1H$ ratio and the standard is the Vienna Standard Mean Ocean Water (V-SMOW).

Large volume stream and possible anthropogenic sulfate source samples were prepared for sulfate sulfur and oxygen isotope analysis. Water samples treated with 3% zinc acetate were filtered through 0.45-micron cellulose nitrate filter paper to remove suspended material. Following filtration, samples were evapo-concentrated down to a one-L volume by heating on a hot plate at below 90°C in a fume hood. Samples were then filtered an additional time through a 0.45-micron filter, rinsed with dilute (~1 N) hydrochloric acid and any precipitate from the concentration was reserved. The filtrate was combined with excess barium chloride (200 g/L) to precipitate all sulfate as barium sulfate ($BaSO_4$). After 24 hr, samples were again filtered through 0.45-micron filter paper, reserving the solid phase on the filter paper. Samples of $BaSO_4$, including the filter paper to avoid sample loss, were then dissolved and purified with a chelating procedure (Diethylenetriaminepentaacetic acid dissolution and reprecipitation or DDARP; Bao, 2006). The reserved evapo-concentration precipitates were also subjected to the DDARP purification procedure to check for lost sulfate during the concentration process. After reprecipitation samples were subjected to a final filtering stage to collect the purified $BaSO_4$ and reserved for future isotopic analysis. In order to test for potential contamination from the filter paper, filter paper blanks were also subjected to the DDARP procedure. Samples contain at most a single filter paper, but it required three filter papers to yield adequate precipitate for isotope analysis, which yield an average concentration of 49 μM oxygen per filter paper from extractions of three, four, and five filter papers. Salt and soil acidifier were dissolved in DI water and prepared for sulfate sulfur and oxygen isotope analysis following the procedure used for stream samples.

Soil, concrete, asphalt, and bedrock iron sulfide deposits were extracted and prepared for sulfate sulfur isotope analysis of operationally defined sulfur pools. Sulfur content (predominantly sulfate) was extracted from asphalt, concrete, and soil. Asphalt and concrete were ground to a fine powder in a shatter box. Soil was dried in a 105°C oven, powered using a hammer, and passed through a 2 mm sieve. Samples of all materials (50–180 g) were extracted using a 0.01M $CaCl_2$ solution with 1:5 mass ratio of sample to solution (Ketterings et al., 2011). Asphalt and concrete solids remaining after the $CaCl_2$ extraction were subjected to an additional extraction with 1 N HCl to extract acid soluble S. Solutions were mixed with a stir bar for 30 min and then allowed to settled overnight before filtration, precipitation, and purification of $BaSO_4$ following the stream water method. Aliquots of the extraction solutions were set aside for IC analysis of sulfate concentration as described above to determine mass of sulfate extracted from the asphalt, concrete, and soil. Iron sulfides were powdered from drill core using a dental drill. Iron or metal sulfide minerals were extracted with the chromium reduction method that recovers reduced S compounds (Canfield et al., 1986). Briefly, samples were placed in a vessel, which was flushed of oxygen with N_2 gas. Sulfide was released from the inorganic sulfides by reaction in boiling, 1M chromium chloride and 3N hydrochloric acid solution and driven by an N_2 carrier gas to a zinc acetate trap, where it formed zinc sulfide. The zinc sulfide was transformed to silver sulfide (Ag_2S) via reaction with silver nitrate, purified by mixing with ammonium hydroxide, and rinsed with deionized water.

For sulfur isotope measurements (S), 0.35–0.45 mg samples of $BaSO_4$ and Ag_2S were weighed into tin boats with 2–4 mg of vanadium pentoxide. For sulfate oxygen isotope measurements ($O_{SO_4^{2-}}$), 0.2–0.25 mg samples of barite were weighed into ashed silver boats in triplicate. Samples were analyzed using an EA Isolink CN elemental analyzer coupled to a Thermo Scientific Delta V Plus continuous-flow isotope ratio mass spectrometer (for sulfur) and a Thermal Conversion Elemental Analyzer coupled to a Thermo Scientific Delta V Plus continuous-flow isotope ratio mass spectrometer (for oxygen) in the Isotope Ratio Mass Spectrometer Lab in the Department of Earth and Planetary Sciences at Johns Hopkins University. The international standards IAEA SO-5, IAEA SO-6, NBS 127, and an in-house barium sulfate standard were used for the $BaSO_4$ samples and

IAEA-S-1, IAEA-S-2, IAES-S-3, and an in-house silver sulfide standard were used for the Ag_2S samples. As with the water isotopes, sulfate sulfur and oxygen compositions were reported in delta notion ($\delta^{34}S$ and $\delta^{18}O_{SO_4^{2-}}$, respectively) as per mil deviations of sample $^{34}S/^{32}S$ and $^{18}O/^{16}O$ ratios from the Vienna Canyon Diablo Troilite and V-SMOW isotope standards, respectively. Standard deviations for the check standards were <0.05‰ ($n \geq 3$).

A correction for filter paper was necessary for the oxygen isotope analyses, but not for the sulfur isotope analyses because we did not detect substantial sulfur in the filter paper extracts. We were only able to detect sufficient oxygen for isotope analysis in extractions of three or more filter papers. The filter paper extracts contained about 40% oxygen by mass with an average $\delta^{18}O$ value of 26.9‰. A contaminant peak was generated in samples containing filter paper, but not in blank or standard analyses. Filter paper extracts were run across several mass values from 0.074 to 0.526 mg to generate a linear relationship between the contaminant peak (A_c) and the signal peak (A_s) area of the oxygen in the filter paper ($A_s = 26{*}A_c - 5.7$, $R^2 = 0.93$). This relationship was used to correct the unknown samples for the filter paper using the contaminant peak area as a proxy for filter paper mass in the unknown sample (average correction of 2.6‰). Similar corrections were not necessary for the sulfur isotope values because the filter paper contains less than 2% sulfur with an average $\delta^{34}S$ value of 3.7‰. Test corrections of sulfur isotope values following the oxygen isotope correction method changed the $\delta^{34}S$ value by less than 0.1‰

Quality control standards were determined based upon the assumption that pure samples of $BaSO_4$ should yield sufficient oxygen and sulfur for isotope analyses in concentrations that are similar to concentrations of these elements in $BaSO_4$. For the oxygen isotope analysis samples with inadequate sample peak area (<40 Vs) were removed. Samples where the calculated contribution of filter paper to the mass of the samples was over 20% were also removed. Oxygen isotope analyses where at least two of the three triplicate sample runs met quality standards were used and the triplicate (or duplicate) results were averaged together to obtain the final value (after Johnston et al. (2014)). For the sulfur isotopes, samples that were less than 11.5 weight % sulfur were removed because this was out of the range of $BaSO_4$ standards measured sulfur concentrations. Nonconsecutive duplicate sulfur isotope analyses were done every 10 samples, and duplicates were averaged together for the final result. While the precipitate collected during evapo-concentration for every sample was analyzed, only three of the evapo-concentration precipitates yielded sulfur or oxygen isotope values. Those precipitate isotope values were similar to the fraction that remained dissolved during concentration with differences of between 0.42 and 1.35‰ for both $\delta^{34}S$ and $\delta^{18}O_{SO_4^{2-}}$ values. A mass balance was used to calculate sulfate sulfur and oxygen isotope values of samples with evapo-concentration precipitates that yielded sulfur or oxygen isotope values. This yielded sulfur and oxygen isotope results for a consistent set of samples.

2.5. Data Analysis

We calculated the annual sulfate flux exported from the forested and suburban catchments. The annual sulfate stream exports were estimated by multiplying the flow-normalized mean sulfate concentration by the total annual discharge:

$$\text{Flow Normalized Mean Concentration} = \frac{\sum_i^n C_i Q_i}{\sum_i^n Q_i} \tag{1}$$

where C_i is each weekly concentration measurement and Q_i is the corresponding discharge value when the stream sample for sulfate analysis was collected. Total annual stream flux was also estimated for the 10th and 90th percentile stream sulfate concentrations to constrain possible uncertainty due to determining the flow-normalized mean concentration value from weekly data.

In order to examine the mobilization of sulfate, we compared actual stream sulfate concentrations during a storm event to those that would be expected under conservative mixing of new water from rainfall and older water stored in the watershed:

$$Q_{\text{total}} = Q_{\text{precip}} + Q_{\text{pre-event}} \tag{2}$$

where Q_{total} is the total volume of stream discharge, Q_{precip} is the volume of stream discharge that is precipitation water, and $Q_{\text{pre-event}}$ is the volume of stream discharge water that was in the catchment before the storm event began, including both antecedent baseflow stream water and groundwater mobilized by the event. And:

$$Q_{\text{total}}C_{\text{total}} = \left(Q_{\text{precip}}C_{\text{precip}}\right) + \left(Q_{\text{pre-event}}C_{\text{pre-event}}\right) \tag{3}$$

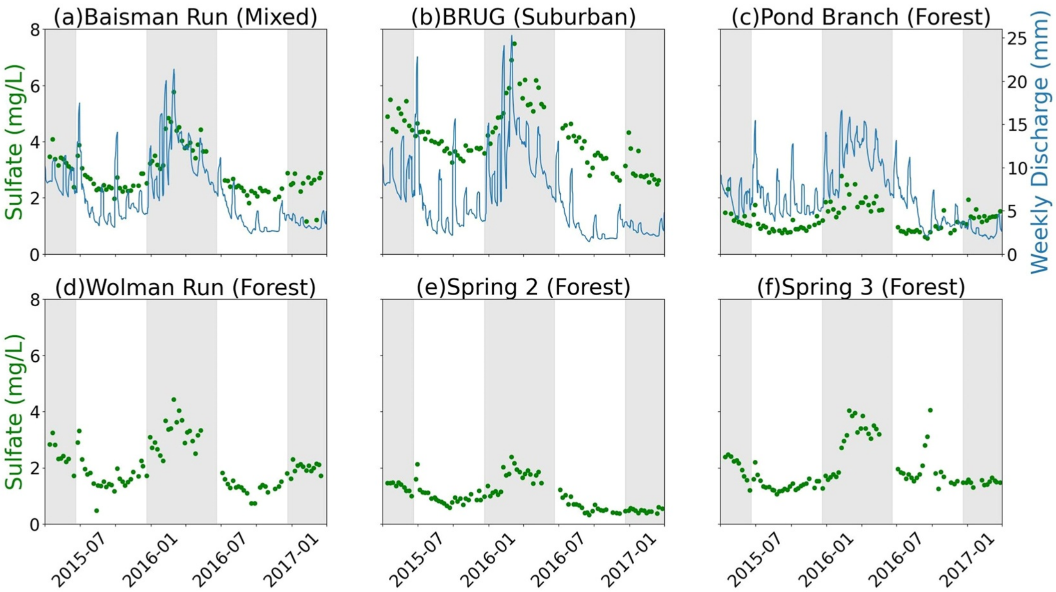

Figure 2. Sulfate concentration (green circles) in weekly grab samples across study sites from April 2014 to April 2017. The 0–8 mg/L range of sulfate concentrations shown on the left *y*-axes is equivalent to a range of 0–83.28 μM. Rolling weekly summed discharge data for gaged catchments (blue lines). Shaded regions denote the winter and spring periods (21 December–20 June). Across sites sulfate concentrations tend to begin to increase in the fall, peak in the winter, and decline during the spring and early summer. While discharge is variable at the storm event scale, the seasonal baseflow discharge signal resembles the pattern in sulfate concentrations.

where C_{total} is the concentration of the conservative solute in the stream, C_{precip} is the concentration of the solute in the precipitation, and $C_{\text{pre-event}}$ is the concentration of the solute in the stream water before the storm event began, which is assumed to be representative of the concentration in groundwater providing stream baseflow (Buttle, 1994). By combining these equations, the streamflow during the storm event was separated into pre-event water and event water using δ^2H values of the precipitation, pre-event stream water, and samples over the course of the event hydrograph (Pinder & Jones, 1969):

$$Q_{\text{pre-event}} = \frac{\left(C_{\text{total}} - C_{\text{precip}}\right)Q_{\text{total}}}{\left(C_{\text{pre-event}} - C_{\text{precip}}\right)} \tag{4}$$

The stream sulfate concentrations for conservative mixing of pre-event stream concentrations and precipitation concentrations were modeled according to the discharge separation using:

$$C_{\text{modeled SO}_4} = \frac{\left(Q_{\text{precip}}C_{\text{precip}} + Q_{\text{pre-event}}C_{\text{pre-event}}\right)}{Q_{\text{total}}} \tag{5}$$

The modeled sulfate concentrations are compared to measurements over the course of the storm event to determine the timing and magnitude of sulfate mobilization to the stream.

3. Results and Discussion

3.1. Stream Sulfate Trends in Space and Time

3.1.1. Seasonal Stream Sulfate Trends

Stream baseflow sulfate concentrations follow a similar seasonal pattern across the forested (PB and Wolman Run), suburban (BRUG), and larger mixed (Baisman Run) catchments (Figure 2), however the amplitude of the seasonal pattern differs with consistently higher suburban stream sulfate concentrations (2.48–7.5 mg/L or 25.8–78.1 μM) than forested stream sulfate concentrations (0.56–2.78 mg/L or 5.83–28.9 μM for PB, Figure 2). Across land use types, weekly stream sulfate concentrations decline over the summer and increase from the

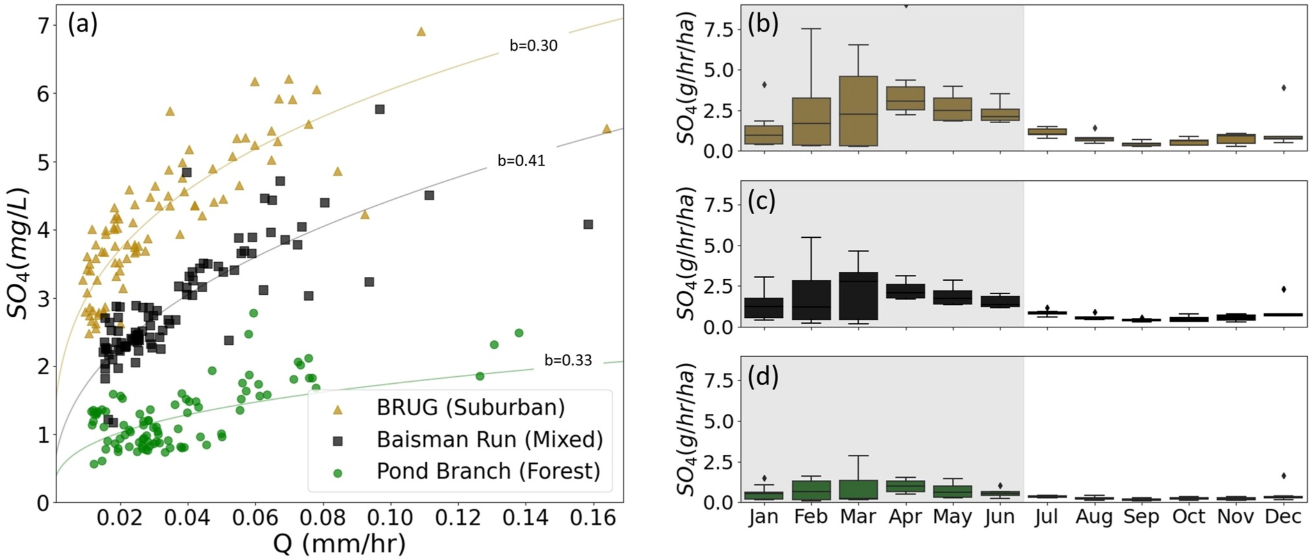

Figure 3. (a) Baseflow concentration discharge relationships for Pond Branch (PB) (forested), Baisman Run (larger mixed land used), and Baisman Run Upper Gage (BRUG) (suburban) catchments. The 0–7 mg/L range of sulfate concentrations shown on the left *y*-axes is equivalent to a range of 0–72.9 μM. Discharge has been area normalized to mm per hour for comparison purposes. All three sites have a positive relationship between stream discharge and sulfate concentrations. Power law fit curves and the corresponding *b*-values have been plotted for each site. Linear regression C-Q relationships for Baisman Run ($r^2 = 0.60$, slope = 26, $p\text{-value} < 0.05$) and BRUG ($r^2 = 0.61$, slope = 31, $p\text{-value} < 0.05$) have steeper slopes than PB ($r^2 = 0.46$, slope = 13, $p\text{-value} < 0.05$). (b, c, and d) Sulfate flux measurements plotted by month and location to show seasonal trend. For all land use types, fluxes are larger during the winter and spring. The seasonal flux increase is larger for watersheds including suburban land use (a, b), compared to the fully forested watershed (c).

winter to early spring. Groundwater discharging from two springs also follows this seasonal sulfate concentration pattern (Figure 2). Wolman Run has higher sulfate concentrations than the other forested sites, which may be related to disruption in this catchment from some selective tree cutting.

The seasonal sulfate trend also strongly corresponds with area-normalized, rolling weekly total stream discharge (Figure 2). Stream sulfate concentrations begin to increase after leaf fall as evapotranspiration decreases and the catchment groundwater storage increases during the cold season. When evapotranspiration increases in the spring and baseflow discharge commensurately decreases, stream sulfate concentrations also decrease. The baseflow concentration-discharge (*C-Q*) relationships also highlights this trend of higher sulfate concentrations during periods of higher stream discharge (Figure 3a). The positive baseflow *C-Q* relationship and seasonality of stream discharge results in substantially higher sulfate fluxes in January–May across land uses (Figures 3b–3d).

3.1.2. Stream Sulfate Trends Across a Storm Event

The concentration dynamics across a storm event differed somewhat from seasonal *C-Q* patterns (Figure 4). The event precipitation had a stable water δ^2H value of −18.7‰ and a sulfate concentration of 0.99 mg/L (10.3 μM). Total precipitation across the discharge record shown was 25.7 mm, with the majority of the precipitation (22.7 mm) occurring from 18:30 to 19:30. The antecedent conditions were typical moist, spring conditions with a smaller precipitation event (<15 mm) two days before the sampled precipitation event. Stream stable water δ^2H values increase in response to the precipitation event and remain fairly elevated as the hydrograph recedes (Figures 4a and 4b). In the suburban hydrograph rising limb and peak of the storm, there is dilution of the sulfate concentration rather than an enrichment that would be expected based upon baseflow seasonal *C-Q* patterns (Figure 4c). This observed initial dilution in stream sulfate matches the prediction of the pre-event and event water mixing model (Figure 4c). The forested stream does not show dilution in the rising limb of the storm hydrograph (in fact a small spike in concentration appears just before the streamflow rises), however forested stream sulfate concentrations are only slightly higher than precipitation concentrations, leading to little change in stream concentration regardless of precipitation water contributions to discharge (Figure 4d).

As the event progresses, sulfate concentrations in both the forested and suburban streams steadily rise. The degree of sulfate enrichment at the end of the period of observation compared to pre-event concentrations is similar between the two catchments and is not explained by conservative mixing of precipitation water and pre-event

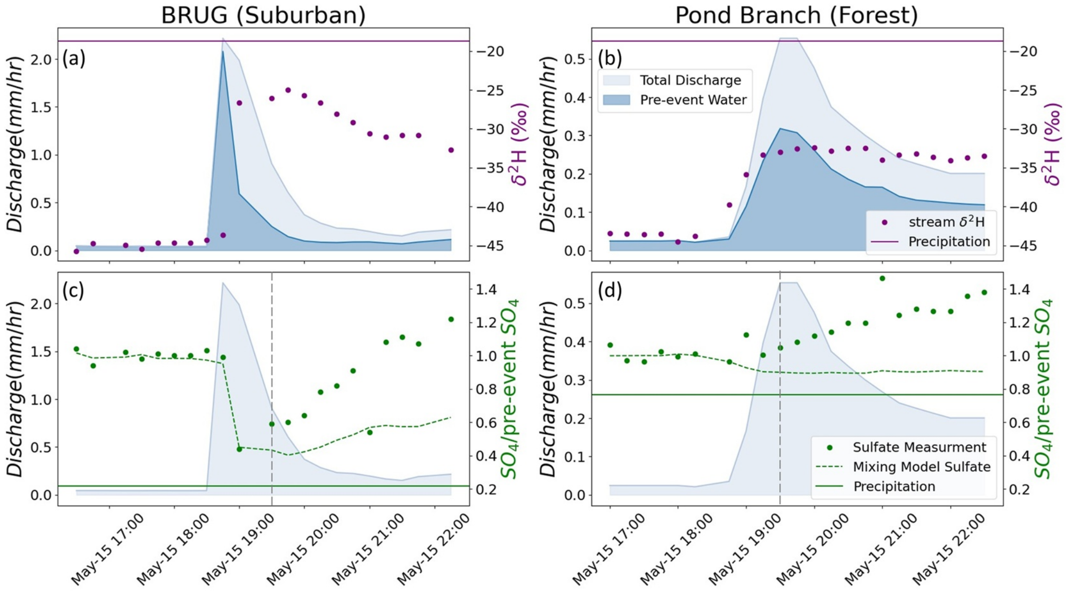

Figure 4. Stream data from a storm event during May 2018. The top row of plots show discharge separated into storm event baseflow and quick flow (left *y*-axis) based upon stable water δ^2H isotopes (right *y*-axis) for the (a) suburban and (b) forested sites. Relevant concentration and isotope values can be found in the text. (c, d) The bottom row of plots shows discharge (left *y*-axis) and measured sulfate concentration dynamics across the event for both sites, along with modeled sulfate concentration ($C_{\text{modeled SO}_4}$) dynamics (right—*y*-axis) based upon a mixing model of the antecedent stream concentrations, precipitation concentrations, and the stable water isotope-based flow separation. Sulfate concentrations are displayed as a ratio with the pre-event stream sulfate concentration to facilitate comparison between the sites. The vertical gray dashed line indicates the detection of enrichment in sulfate concentrations. The δ^2H value of precipitation and the ratio of the precipitation sulfate concentration to the pre-event stream sulfate concentration are displayed as solid horizontal lines for reference.

water concentrations (Figure 4). The suburban stream sulfate enrichment is initiated during the falling limb of the storm hydrograph (Figure 4). In contrast, the forested stream sulfate enrichment appears to be initiated during the late rising limb or peak of the storm hydrograph (Figure 4). This difference in timing of sulfate enrichment initiation with respect to the hydrograph between the forested and suburban streams may be the result of runoff from impervious areas causing the suburban streams hydrograph to peak and recede more quickly than the forested stream event hydrograph (Figure 4). The dilution observed in the suburban stream around peak discharge would be consistent with this runoff having a sulfate concentration identical to rainfall, implying that it did not mobilize any sulfate stored in the landscape. Stream sulfate concentrations in both the forested and suburban streams appear to have a similar lag (~1 hr) following the initiation of the storm event and similar magnitude of relative enrichment compared to antecedent concentrations (Figure 4d).

3.1.3. Sulfate Storage and Mobilization to the Stream: Soil Sulfate

The similar timing of storm event stream sulfate enrichment in both forested and suburban watersheds as well as the seasonal trends of increasing sulfate with discharge at all sites suggest that the timing of sulfate enrichment is not related to source application to the landscape, but rather the nature of sulfate storage and release in the catchment. Mobilization of sulfate during seasonal and event-scale wetter periods may result from a surface or shallow subsurface source. The lag in enrichment during storm events suggests that this sulfate source is not directly adjacent to the stream, and not associated with runoff from impervious areas.

Soil samples from the ridge in the forested watershed contain an average of 15.9 mg sulfate per kg soil and a maximum of 32.7 mg sulfate per kg soil in samples collected down to 160 cm (Table 2). Soil sulfate concentrations appear to be largest in the top 50 cm and decrease somewhat with depth (Table 2), however soil sulfate storage at greater depths was not sampled. Estimating the magnitude of the total extractable sulfate in the top meter of soil based upon that average value yields 210 kg of soil-stored sulfate per hectare in the top meter of soil in the forested watershed (Appendix Table E in Supporting Information S1). Considering the thick regolith and literature findings that legacy sulfate stores have been large and slow to elute from non-glaciated piedmont landscapes (Rice et al., 2014), this soil-stored sulfate for the top meter is likely much smaller than the total store

Table 2
Extracted Sulfate Masses From Pond Branch Soil and Local Concrete and Asphalt Samples

Sample (depth below surface)	Extraction	Mass sulfate (mg SO_4/kg sample)
PB soil (0–10.2 cm)	$CaCl_2$	27.9
PB soil (40.6–45.7 cm)	$CaCl_2$	32.7
PB soil (58.4–67.3 cm)	$CaCl_2$	18.3
PB soil (86.4–91.4 cm)	$CaCl_2$	10.2
PB soil (106.7–113 cm)	$CaCl_2$	0
PB soil (127–132 cm)	$CaCl_2$	9.9
PB soil (157.5–163.8 cm)	$CaCl_2$	12.4
Concrete	$CaCl_2$	122.6
Concrete	HCl	177.3
Asphalt	$CaCl_2$	210.5
Asphalt	HCl	18.4

Note. The soil, concrete, and asphalt were extracted using a $CaCl_2$ solution. A second extraction was performed on the concrete and asphalt samples using a HCl solution. Soil sulfate concentrations tend to decrease with increasing depth below the surface. Concrete and asphalt samples contain substantial sulfate, though it is worth noting that samples were crushed before extraction, exposing fresh surfaces.

of sulfate in the thick soil and saprolite. Mobilization of sulfate in forest soils has long been considered a major source to the stream (Cosby et al., 1986) and appears to be rate limited by contact time of water with soil controlling dissolved sulfate concentrations (Cai et al., 2011; Selim et al., 2004). The similarity between temporal dynamics of sulfate flux in the forested and suburban catchments suggests that the suburban catchment has similar mobilization of soil sulfate stores even though the total mass of subsurface sulfate is likely much larger in the suburban catchment (see below).

3.2. Sulfate Budget

3.2.1. Sulfate Budget, Forest

Stream sulfate flux and source contribution budgets were estimated for the catchments to gain insights into the cause of the larger suburban sulfate fluxes, despite the similar mobilization dynamics. Annual stream sulfate fluxes for the 2-year period from April 2015 to March 2017 in the forested catchment were estimated to be ∼5 kg of sulfate annually per hectare compared to ∼16.6 kg/ha annually for the suburban catchment (Table 3). The annual suburban stream flux is larger even when comparing the estimate based upon the 10th percentile concentration for the suburban stream (9.7 kg/ha) to that for the 90th percentile concentration for the forested stream (6.5 kg/ha). These annual stream fluxes are small in comparison to the estimated magnitude of the soil sulfate pool of over 200 kg/ha.

Geologic sources, historic land use, and (particularly historical) atmospheric deposition were considered as possible sulfate contributors in the forested catchment. There is very little geogenic sulfur present in minerology studies of the site and rock core observations, likely making it a minor source (Cleaves et al., 1970). The iron sulfides in the rock core were primarily found within highly resistant quartz veins. In terms of land use, the PB watershed has been continuously natural forest with some selective logging pre-1958 (Cleaves et al., 1970). Nothing in the history of the forested catchment suggests that additional legacy sources beyond atmospheric deposition are likely to contribute sulfate. Atmospheric deposition in the region has been declining since 1990 and was quantified to be approximately 5–7 kg per hectare sulfate during the period of study (Eng & Scanlon, 2021). Thus, atmospheric deposition can explain current sulfate fluxes in the forested catchment though it should be noted that on the decadal scale, sulfate concentrations in PB are decreasing more slowly than the decrease in precipitation (0.6 and 1.8 mg/L decreases, respectively, from 1999 to 2014, Bird et al., 2018).

Table 3
Sulfate Flux Estimates for the Gaged Forested Catchment (Pond Branch) and Suburban Catchment (Baisman Run Upper Gage)

Sulfate flux	Pond branch (forest) (kg/ha/yr)	BRUG (suburban) (kg/ha/yr)
Stream exports	−5 (−2.8, −6.5)	−16.6 (−9.7, −19.4)
Atmospheric deposition	5–7	5–7
Road salt	N/A	0–0.06
Human effluent (septic)	N/A	3.3–6.6
Surfactants (detergents, etc.)	N/A	2.2–4.4
Lawn/garden care	N/A	0.3–4.3
Infrastructure	N/A	0–0.03
Legacy agricultural use	N/A	Unknown

Note. Catchment export in stream flow is given as a negative flux and inputs from sulfate sources to the catchments are listed as positive. The stream exports are estimated based upon flow weighted mean concentration values. The stream flux value range calculated using 10th and 90th percentile concentrations are provided parenthetically.

Cleaves et al. (1970) published a geochemical mass balance for PB that also concluded that the sulfate inputs can be attributed to atmospheric deposition, though the sulfate deposition rate was much higher than the sulfate flux at the time. Atmospheric sulfate inputs were 17.84 kg/ha/yr in the mid-1960s (Cleaves et al., 1970), whereas atmospheric deposition of sulfate has declined by 70%–90% since the 1990 Clean Air Act Amendment (Eng & Scanlon, 2021). Despite large atmospheric contributions, Cleaves et al. (1970) measured very similar mean PB baseflow concentrations of 1.3 mg/L or 13.5 μM (1.26 mg/L or 13.1 μM is Figure 2 mean) and estimated an annual stream flux of 3.93 kg/ha/yr. It is worth noting that the Cleaves et al. (1970) study occurred during a historic drought period and that they reported peak stream sulfate concentrations during storms as averaging 6.3 mg/L (65.6 μM), substantially higher than the maximum sulfate concentration recorded during this study. Thus, the forested sulfate stream flux during the Cleaves et al. (1970) study may have been lower than our annual stream flux (5 kg/ha) even with the much higher atmospheric inputs because the time period of the study was drier and had lower annual stream discharge (160 mm/yr in the Cleaves et al. study compared to 350 mm/yr during this study). The sulfate budget in Cleaves et al., concluded that >12 kg/ha/yr were accumulating in the forested catchment (1970). The contrast between stream sulfate fluxes in the 1960s and more recently suggest that regardless of the rate of atmospheric loading, the rate of mobilization is related to wetness conditions, particularly the magnitude of annual streamflow.

3.2.2. Sulfate Budget, Suburban

Atmospheric deposition rates of sulfate are likely similar between the forested and suburban catchment due to their proximity. Major forms of atmospheric deposition include wet deposition, "acid rain," and dry deposition of atmospheric particulates onto surfaces (Lindberg et al., 1986). Catchments in the same region are exposed to the same general atmospheric sulfate concentrations and precipitation, leading to approximately identical rates of wet deposition (Likens & Bormann, 1974). Dry deposition is also likely to be similar across neighboring catchments, however it may partially depend upon the surface area available for particles to collect (Davidson et al., 1985). Due to the leaf canopy, forested catchments have larger surface areas compared to suburban catchments with the same footprint and thus are expected to have higher rates of dry deposition (Lindberg et al., 1986). Therefore the 5–7 kg/ha/yr estimated range of annual atmospheric sulfate deposition is a maximum range estimate for the suburban catchment.

The suburban catchment exported an estimated 16.6 kg of sulfate annually per hectare resulting in a suburban excess of 11.6 kg annually per hectare compared to the atmospheric deposition rate and the forested catchment. Maximum and minimum sulfate fluxes and contributions by possible suburban sources were estimated to constrain the bounds of possible sources of suburban sulfate. Estimates are approximate due to scarcity of data but are still useful for investigating which sources contribute loads that approach the order of magnitude of stream exports. Sources considered include road salt, septic effluent, lawn and garden care products, infrastructure, and legacy sources from historic land use.

Road salt was explored as possible sources of suburban sulfate as sulfate is a trace constituent of halite evaporite deposits (Dean et al., 1987). Local road salt has been measured to be approximately 60 ppm sulfate (Price & Szymanski, 2014) and the state policy suggests applying 2,903 kg of road salt per lane mile per storm (Strachan et al., 2009). BRUG contains approximately one lane mile of state road and 55 homes based upon geospatial analysis in Google Earth. Salt sulfate contribution estimates are negligible (0.06 kg/ha) despite using a large maximum estimate of 10 salting events and assuming homeowners each apply large amounts of road salt at 100 kg annually (Table 3, Appendix Table A in Supporting Information S1 for further detail).

Homes in the suburban catchment use septic fields which receive human waste and cleaning supplies used in the household that contain multiple sulfur species (McAvoy et al., 2009; Wilhelm, Schiff, & Cherry, 1994). Documented instances of connection between Piedmont septic fields and streams combined with evidence that septic field redox processes may favor sulfate production suggest that septic waste may be an important source of stream sulfate. Properly functioning septic fields include unsaturated and saturated zones that support complex biogeochemical cycling intended to treat wastewater (Gayle et al., 1981; Wilhelm, Schiff, & Cherry, 1994; Wilhelm, Schiff, & Robertson, 1994). Studies in the Northern Carolina Piedmont have demonstrated that the nutrients nitrate and phosphate may be incompletely removed by septic fields and can increase solute concentrations in nearby stream water (Humphrey et al., 2016; Iverson et al., 2018). Although data on sulfate dynamics in septic fields are scarce, one study found sulfate concentrations were elevated in the aerobic zone of a septic field where sulfur in organic waste material was oxidized to sulfate (Wilhelm, Schiff, & Cherry, 1994). Additionally, a study of denitrification in a septic plume in a pyrite-containing sandy aquifer in Canada found that reduced sulfur can act as an electron donor in denitrification of septic waste, becoming oxidized to sulfate (Aravena & Robertson, 1998).

Maximum and minimum septic field sulfate excreted by humans in the catchment was estimated. The BRUG catchment contains 55 homes and we assumed between 2 and 4 residents per home. Limited data is available on sulfur excreted by humans, but measurements from adult men suggest mean values of 2.9 g/day in urine sulfur losses and <0.05 g/day in fecal loses (Magee et al., 2000). This may be an overestimate for the general population, as sulfur loss is correlated with intake in diet (Magee et al., 2000), but should offer an estimate of the upper bound of possible fluxes. We assumed no sulfur was retained by the septic tank since the majority of sulfate in human effluent is dissolved. This suggests human effluent may contribute between 3.3 and 6.6 kg/ha/yr sulfate (Table 3, Appendix Table B in Supporting Information S1 for further detail).

Sulfur is present in many personal care and cleaning products and detergents, largely as a surfactant. The two most common sulfur-bearing surfactants in household products are linear alkylbenzene sulfonate and alcohol ether sulfate which includes sodium lauryl sulfates (Nielsen et al., 2009). Measurements of septic tank effluent from a 4-person household have found mean concentrations of 14.6 mol/L linear alkylbenzene sulfonate and 4.8 mol/L alcohol ether sulfate (Nielsen et al., 2009). We estimated 1,000 L of daily wastewater discharge for a 4-person household based upon the high end of EPA personal wastewater volume estimates (USEPA, 2002). These values produce an annual surfactant sulfur contribution as sulfate of up to 4.4 kg/ha (Table 3). The minimum value for a 2-person household was estimated as half of the flux from the 4-person household calculation. Septic fields have been demonstrated to successfully break down surfactants, so it is possible most sulfur would exit the drain field as sulfate (Nielsen et al., 2009; Shimp et al., 1994). Combined with the human excrement sulfate sources, total maximum septic sources can almost account for the total suburban excess with 11 kg/ha (Table 3), assuming that the estimates are not too generous and most sulfur from wastewater ultimately reaches the stream as sulfate.

Sulfur is found in several lawn and garden care products including soil acidifier, fertilizer, and fungicide. We estimated sulfate flux based upon fertilizer contributions as other products are much less widely applied to the suburban landscape. A regional study found median fertilizer application rates of 28.5 kg/ha/yr (Fraser et al., 2013). Popular commercial household fertilizers' packaging claim between 1% and 10% sulfur so the minimum and maximum fluxes were estimated based upon these values. Between 30% and 50% of the land use in the BRUG catchment is occupied by lawns (Figure 1). We estimated a range of 0.3–4.4 kg/ha as sulfate equivalents of the sulfur applied annually (Table 3, Appendix Table C in Supporting Information S1 for further detail).

Many building and suburban infrastructure materials contain sulfur. Rubble from building materials, particularly gypsum wallboard and plaster, has been demonstrated to release substantial sulfate (Abel et al., 2015). However, it is not clear whether intact buildings produce a significant sulfur flux. BRUG is a very low density suburban development dating to the 1970s (Hill, 1969), so substantial amounts of buried infrastructure or rubble are unlikely. Exterior materials known to contain sulfur include brick, concrete, and asphalt. Brick contains up to 2 g of sulfur per kg, however brick materials in soils tend to act as sulfate sinks rather than sources (Nehls et al., 2013). Asphalt in roads and roofing materials and concrete appear to have the largest exposed surface area of infrastructure materials in the catchment. We estimated a combined road, driveway, and roof surface area in BRUG of 840 m^2/ha (Appendix Table D in Supporting Information S1 for further detail). The annual mass of infrastructure materials dissolved is unknown, but a range of 0–100 g of dissolved material per square meter of infrastructure surface area annually was used to estimate the possible order of magnitude. Degradation and leaching of asphalt and concrete have been demonstrated to produce sulfate (Huang et al., 1995; Jacques et al., 2010). Leaching experiments produced 300 mg total of sulfate/kg of concrete and 230 mg total of sulfate/kg of asphalt (Table 2). Using the max leaching value of 300 mg sulfate per kg infrastructure based on concrete, we estimate a maximum contribution of 0.03 kg sulfate/hectare (Table 3). While some sulfate may be contributed by building materials, it is unlikely that this contributes substantially to the excess suburban stream sulfate.

Finally historic land use may result in legacy sulfate sources. The BRUG catchment had a similar selective logging land use in the mid-1800s but transitioned to agricultural land use in part of the catchment around 1870 (Baltimore Sun, 1969). In the late 1960s, BRUG began to be converted into suburban home parcels (Hill, 1969). Agricultural land use was described as primitive with few livestock and “old-time” growing methods that likely did not involve heavy application of fertilizer (Baltimore Sun, 1969), but historic records are scarce. During approximately a century of agricultural land use, fertilizer, and livestock may have contributed some sulfate to the landscape. Legacy agricultural sulfate may still be present in the soil and contribute sulfate to the stream in the suburban catchment but is difficult to quantify. Legacy land use that exceeds 50 years cannot be disregarded because long-term lag in exporting legacy atmospheric deposition has been observed in the southern Piedmont (Eng & Scanlon, 2021; Patel et al., 2020; Rice et al., 2014).

Despite the uncertainties in the sulfate budget necessitating large ranges of source flux estimates, none of the maximum estimates for suburban sulfur sources can independently account for the sulfate flux in the suburban catchment that is excess of the forested catchment flux (Table 3). The suburban catchment exporting over three times the sulfate flux from the forested watershed is the combined effect of additional sulfur inputs from multiple sources (Table 3). Road salt contributes only minor sulfate, though it is a substantial source of pollution for chloride and other ions with concerning ecological impacts (Table 3, Hintz & Relyea, 2019). However, human effluent, surfactants in household and personal care products, and lawn care products could contribute

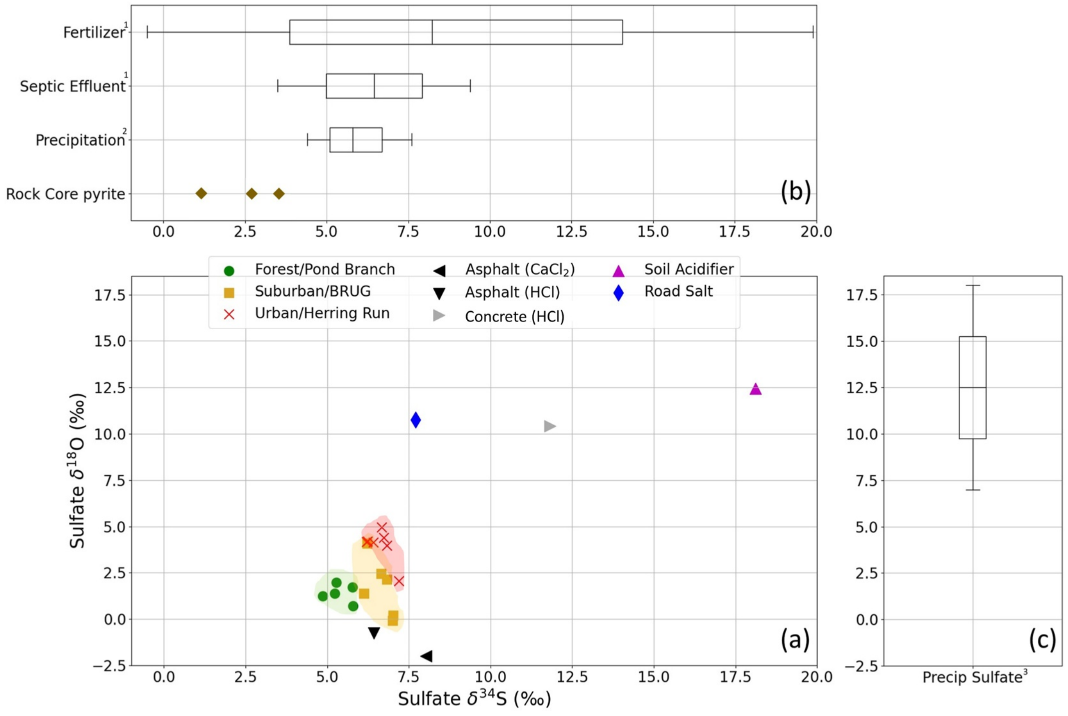

Figure 5. (a) Scatter plot comparing sulfate δ^{34}S and sulfate $\delta^{18}O_{SO_4^{2-}}$ values precipitated from forested (Pond Branch [PB]), suburban (Baisman Run Upper Gage), and urban (Herring Run) catchments, along with sampled sources. The forested, suburban, and urban stream value regions have been highlighted in green, yellow, and red, respectively. Herring Run sulfate concentrations ranged from 15.6 to 27.9 mg/L (162–290 μM) during the period where samples were collected for stream sulfate isotope analysis. Uncertainties not shown because of small error bar size relative to symbol size. (b) The ranges of δ^{34}S values for sulfur sources from literature and values measured for pyrite in the PB catchment are displayed. Fertilizer δ^{34}S values are from [1]Cravotta, (1995) and regional precipitation δ^{34}S values range are from [2]Cooney, 2005). Plot (c) shows a literature range for atmospheric deposition sulfate $\delta O_{SO_4^{2-}}$ ([3]Krouse & Mayer, 2000).

substantial sulfur and have maximum fluxes of a similar order of magnitude (Table 3). Other potential sources including legacy low-intensity agricultural land use and the impact of building and infrastructure materials in this low-density suburban development likely contribute smaller amounts of sulfur (Table 3). Narrowing down the relative importance of suburban sulfate sources to the stream requires further information beyond the budget results.

3.3. Stream and Source Sulfate Isotope Tracers

Given the uncertainty in the relative magnitude of different suburban sulfate sources to the stream, sulfate sulfur (δ^{34}S) and oxygen ($\delta^{18}O_{SO_4^{2-}}$) isotope values may be able offer additional insights as source tracers. To aid in the analysis of how stream water sulfate δ^{34}S and $\delta^{18}O_{SO_4^{2-}}$ values reveal information about sulfate sources and mobilization, we compare the forested and suburban stream to an urban stream in the region (West Branch of Herring Run). The forested stream had slightly lower sulfate δ^{34}S values ranging from 4.9 to 5.8‰ ($n = 5$) compared to the suburban stream range of 6.1–7.0‰ ($n = 6$) and the urban stream range of 6.2–7.2‰ ($n = 7$), with a significant difference between the forested mean values and the mean values for the other catchments (t-test $p < 0.0005$, Figure 5). Stream $\delta^{18}O_{SO_4^{2-}}$ values were more variable than the δ^{34}S values, ranging from 0.7 to 2.0‰ in the forested stream, from −0.1–4.1‰ in the suburban stream, and from 2.1 to 5.0‰ in the urban stream (Figure 5). Forested and suburban stream mean $\delta^{18}O_{SO_4^{2-}}$ values were not significantly different, but both forested and suburban mean $\delta^{18}O_{SO_4^{2-}}$ values were significantly lower than the urban stream $\delta^{18}O_{SO_4^{2-}}$ mean ($p < 0.05$). Forest stream $\delta^{18}O_{SO_4^{2-}}$ values had a narrower range (1.3‰) than the suburban (4.2‰) and urban (2.9‰) streams. The differences in sulfate isotope value signatures across land use may help identify sulfate sources that contribute to each stream.

Stream sulfate sulfur and oxygen isotope values may be impacted by (a) the isotopic composition of the source sulfate, (b) mixing and, and (c) fractionation effects from biogeochemical cycling (Kester et al., 2003; Mayer et al., 1995; Shanley et al., 2005). In some cases, sulfate oxygen and sulfur isotope ratios have been demonstrated to behave conservatively in riverine systems (Burt et al., 2021). However, sulfate delivered to streams may have undergone several processes: soil adsorption and desorption (Rajan, 1978), microbially mediated reduction of sulfate coupled oxidation of organic matter under anoxic conditions (i.e., microbial sulfate reduction or MSR; Tuttle et al., 1969), reoxidation of the MSR product sulfide, biological uptake, and release during remineralization of organic matter (David & Mitchell, 1987). Soil adsorption and desorption are likely to be prevalent at our study site given the size of the soil sulfate pool and sulfate mobilization by wet conditions noted above (Figure 2). Adsorption and desorption do not cause significant sulfate sulfur or oxygen isotope fractionations and should not impact isotopic signatures (Van Stempvoort et al., 1990).

However, several of the other biogeochemical processes can fractionate sulfate sulfur and oxygen isotopes. MSR can have a large impact on sulfate isotope and signatures, with a sulfur isotope fractionation of up to 70‰ (Sim et al., 2011) and an oxygen isotope fractionation up to 30‰ (Farquhar et al., 2008). Sulfide oxidation can result in a smaller sulfur isotope fractionation of ∼−5 to 5‰ at neutral pH (Pellerin et al., 2019), and the reoxidation of sulfide is often complete in well-oxygenated settings, resulting in no net sulfur isotope fractionation. However, the reoxidation of sulfide can reset the oxygen isotope of sulfate to a value that is ^{18}O-enriched by up to 20–30‰ relative to $\delta^{18}O_{H_2O}$ values of water (Aharon & Fu, 2000; Antler et al., 2013; Fritz et al., 1989; Mizutani & Rafter, 1969). The sulfur δ^{34}S fractionation associated with biological uptake and remineralization is minor (0.5 ± 2.4‰, Kaplan & Rittenberg, 1964; Nehlich, 2015), while the sulfate $\delta^{18}O_{SO_4^{2-}}$ isotope fractionation is substantial with depletion of 4.5–6.3‰ due to sourcing oxygen during remineralization from the ^{18}O-depleted water (Kester et al., 2003; Mayer et al., 1995; Shanley et al., 2005). Therefore, excluding substantial net MSR, sulfur isotope signatures should reflect source values, but oxygen isotope values may be affected by biological processes.

Several potential sulfate sources have δ^{34}S ranges that overlap with stream sulfate δ^{34}S values (Figure 5). Precipitation and forested soil sulfate concentrations were too low to extract adequate sulfate for isotopic analysis. However, the mean regional precipitation literature sulfate δ^{34}S value (5.8‰, Cooney, 2005) resembles the mean forested stream value (5.4‰). The $CaCl_2$ and HCl extractions of concrete yielded similar δ^{34}S values of 11.9 and 11.8‰, respectively, while the same successive extractions of asphalt yielded δ^{34}S values of 8.0 and 6.4‰, respectively. Road salt and soil acidifier also have higher δ^{34}S values compared to the stream water sulfate. In contrast, the metal sulfide samples from the rock core have lower δ^{34}S values (1.2–2.7‰). Septic effluent influenced streams and fertilizer values from literature have sulfate δ^{34}S ranges that overlap with mean values of stream sulfate in the suburban and urban catchments (Cravotta, 1995). With the possibility of mixing of multiple sources of sulfate and overlapping source isotopic values, sulfur isotopes alone cannot clearly distinguish suburban and urban sulfur sources.

While suburban sources could not be clearly distinguished by sulfate isotope tracers, each of the stream sites does have a relatively narrow range of sulfate δ^{34}S values (Figure 5). The similarity between forested stream sulfate and atmospheric deposition sulfate δ^{34}S values provides evidence that atmospheric deposition is the main source of sulfate and thus that little fractionation of sulfur isotopes occurs in this system (Figure 5). Sulfur isotope fractionation associated with MSR is likely limited because of oxic soil conditions and preferential remineralization of organic matter through other thermodynamically favored oxidants (e.g., nitrate or iron oxides). The slight ^{34}S-depletion in the mean δ^{34}S value of forested stream sulfate relative to precipitation could be due to a small contribution from metal sulfides, but many of the measured values are indistinguishable from precipitation δ^{34}S value and metal sulfides are not abundant in the bedrock (Cleaves et al., 1970). Given that the forested stream δ^{34}S values indicate that the main source of sulfate is precipitation, higher δ^{34}S values in sulfate in the suburban and urban stream reflect the addition of anthropogenic sulfate sources with higher δ^{34}S values (i.e., fertilizer, septic effluent road salt, acid-soluble S in concrete, or soil acidifier).

Sulfate oxygen isotope values have a narrow range at the forested site and across most urban samples but vary more widely at the suburban site. Both forested and suburban stream water $\delta^{18}O_{H_2O}$ values are around −7‰. Equilibrium oxygen isotope exchange between sulfate and water occurs over long time-scales (∼10^7–10^9 years at neutral pH and room temperature, Lloyd, 1968; Zak et al., 1980). However, equilibrium oxygen isotope exchange between the sulfur intermediate sulfite and water can occur rapidly during microbial sulfate reduction and/or sulfide oxidation reactions, resulting in the production of sulfate that is ^{34}S-enriched relative to water by up to 30‰ (Aharon & Fu, 2000; Antler et al., 2013; Fritz et al., 1989; Mizutani & Rafter, 1969). Thus, sulfate recycled from metabolic intermediates from microbial sulfate reduction (Farquhar et al., 2008) or sulfide oxidation could have a $\delta^{18}O_{SO_4^{2-}}$ value as high as 23‰, which is lower than the stream $\delta^{18}O_{SO_4^{2-}}$ values (Figure 5). Local atmospheric deposition sulfate $\delta^{18}O_{SO_4^{2-}}$ values have not been measured, but atmospheric $\delta^{18}O_{SO_4^{2-}}$ values can range from 7 to 18‰ (Krouse & Mayer, 2000). The measured stream $\delta^{18}O_{SO_4^{2-}}$ values are below the atmospheric $\delta^{18}O_{SO_4^{2-}}$ value range, as well as the majority of anthropogenic sulfate sources excluding HCl-soluble sulfate from asphalt (Figure 5). The intermediate stream values between likely atmospheric deposition and anthropogenic sulfate values and stream water values suggest that some of the sulfate comes from the remineralization of organic sulfur. Remineralization of assimilated sulfur results in the production of sulfate with low oxygen isotopes values because the oxygen comes from ambient water with minimal isotopic fractionation (Kester et al., 2003; Mayer et al., 1995; Shanley et al., 2005). This process could also occur in septic systems and may be more likely due to the oxic soil conditions and relative lack of sulfide sulfur sources (see budget sections).

Differences in the range of $\delta^{18}O_{SO_4^{2-}}$ values across land uses may indicate differences in the degree of biological sulfate cycling and/or the input of anthropogenic sulfate with high $\delta^{18}O_{SO_4^{2-}}$ values (Figure 5). The lower values at the forested site suggest that a greater portion of the sulfate in the forested site passes through organic matter compared to the urban site (Figure 5). This difference could also result from higher $\delta^{18}O_{SO_4^{2-}}$ values of concrete (10.4‰) if it is a major urban source (Figure 5). The suburban site stream $\delta^{18}O_{SO_4^{2-}}$ values overlap with both the forested and urban sites. The lower suburban stream $\delta^{18}O_{SO_4^{2-}}$ values may be associated with warmer months, with samples from June and July having values of 0.21 and −0.07‰ respectively, while the higher values (2.1–4.1‰) are from March through early May. It is possible that there is greater biological cycling in the suburban catchment in the warm season, leading to greater ^{18}O-depletion, however the data is limited. The ^{18}O-depletion of sulfate due to microbial sulfate assimilation and remineralization likely occurs in the shallow soil (Mayer et al., 1995), which corroborates the conclusion that the sulfate mobilized to the stream by wet conditions in the forested and suburban catchments is first stored in the soil. Thus, while anthropogenic sulfate sources increase sulfate concentrations in suburban streams, the processes of remobilization are similar across land-use types.

4. Conclusions

The environmental gains of the last few decades that have resulted from decreased atmospheric sulfate inputs to freshwater systems may be offset by inputs from anthropogenic sulfate sources in (sub)urban systems. Here we present sulfate concentration and isotope data and interpret them with respect to changes in discharge and catchment sulfate budgets to investigate sources and styles of mobilization of sulfate in unglaciated forested versus suburban catchments. Seasonal and storm event mobilization and transport of sulfate to the streams vary in time in similar ways between the forested and suburban catchments (Figures 2 and 4) but differ in magnitude. The positive correlation between stream discharge and sulfate concentrations in the seasonal data set, along with the lag in enrichment until after the peak in stormflow suggests that sulfate is mobilized from shallow storage by wet conditions, rather than being mobilized by runoff from impervious surfaces. The relatively large size of the soil sulfate pool compared to annual stream sulfate fluxes and $\delta^{18}O_{SO_4^{2-}}$ signature of shallow biological soil process in the stream sulfate also supports the role of shallow sulfate storage in both forested and suburban catchments. Soil sulfate mobilization may occur through desorption while in contact with infiltrating precipitation water and rising water tables.

Though the sulfate storage and transport mechanisms appear to be similar between the forested and suburban watersheds, anthropogenic inputs from several sources result in elevated sulfate in the suburban catchment, resulting in higher stream sulfate concentrations and fluxes. Mass balance estimates suggest that the larger flux of sulfate in the suburban landscape is the result of multiple source contributions. Many of the sulfate sulfur and oxygen isotope values of sulfate sources overlap, which hampers our ability to model the relative fraction of suburban stream sulfate from each source. Nevertheless, our estimates of annual fluxes from potential anthropogenic sources indicates that septic systems and fertilization are the most likely contributors, which is consistent with the sulfate sulfur and oxygen isotope data, and that road salt sulfate contributions are minor. The diffuse, non-point source nature of these sulfate sources suggests that reducing suburban sulfate fluxes would be challenging. Efforts have been made to reduce fertilizer application rates (Fertilizer Use Act, 2011) and sulfate-free personal care products are gaining some popularity. However, our characterization of sulfate fluxes and transport dynamics suggests suburban land use sulfate contributions are substantial and may require further efforts to mitigate.

Data Availability Statement

The geochemical and hydrological data used in the study are available at the Johns Hopkins University Data Archive (https://archive.data.jhu.edu) via https://doi.org/10.7281/T1/NU0VS7 (Cosans et al., 2024).

Acknowledgments
This research was funded by National Science Foundation Grants EAR-1654194 and EAR-2012264 (CJH), ICER/RISE-1540631, and EAR-2012313 (JM). This research also was funded by the U.S. Geological Survey (USGS) under Grant/Cooperative Agreement G16AP00061, Subawards 79176-Z9212105, and 81425-Z9212106 (MG, JM). Its contents are solely the responsibility of the authors and do not necessarily represent the official views of the USGS. The authors thank Dana Brenner for tremendous help with the sulfate sulfur and oxygen isotope analysis and Ben Gill for help with initial sulfur isotope analyses. The authors also thank Kalev Hantsoo for help sample processing and Ian Yesilonis and Rui Jin for help with sampling of soil cores and water, as well as helpful discussions. The authors also thank Shane Putnam for incredible help establishing field site infrastructure and for collecting water samples, and David Litwin for assistance creating the site map.

References

Abel, S., Nehls, T., Mekiffer, B., Mathes, M., Thieme, J., & Wessolek, G. (2015). Pools of sulfur in urban rubble soils. *Journal of Soils and Sediments*, *15*(3), 532–540. https://doi.org/10.1007/s11368-014-1014-1

Aharon, P., & Fu, B. (2000). Microbial sulfate reduction rates and sulfur and oxygen isotope fractionations at oil and gas seeps in deepwater Gulf of Mexico. *Geochimica et Cosmochimica Acta*, *64*(2), 233–246. https://doi.org/10.1016/s0016-7037(99)00292-6

Antler, G., Turchyn, A. V., Rennie, V., Herut, B., & Sivan, O. (2013). Coupled sulfur and oxygen isotope insight into bacterial sulfate reduction in the natural environment. *Geochimica et Cosmochimica Acta*, *118*, 98–117. https://doi.org/10.1016/j.gca.2013.05.005

Aravena, R., & Robertson, W. D. (1998). Use of multiple isotope tracers to evaluate denitrification in ground water: Study of nitrate from a large-flux septic system plume. *Groundwater*, *36*(6), 975–982. https://doi.org/10.1111/j.1745-6584.1998.tb02104.x

Baltimore Sun. (1969). *May dates set for farm tour*. The Baltimore Sun.

Band, L. E., Tague, C. L., Groffman, P., & Belt, K. (2001). Forest ecosystem processes at the watershed scale: Hydrological and ecological controls of nitrogen export. *Hydrological Processes*, *15*(10), 2013–2028. https://doi.org/10.1002/hyp.253

Bao, H. (2006). Purifying barite for oxygen isotope measurement by dissolution and reprecipitation in a chelating solution. *Analytical Chemistry*, *78*(1), 304–309. https://doi.org/10.1021/ac051568z

Bird, D. L., Groffman, P. M., Salice, C. J., & Moore, J. (2018). Steady-state land cover but non-steady-state major ion chemistry in urban streams. *Environmental Science & Technology*, *52*(22), 13015–13026. https://doi.org/10.1021/acs.est.8b03587

Blaszczak, J. R., Delesantro, J. M., Zhong, Y., Urban, D. L., & Bernhardt, E. S. (2019). Catchment urban development controls on urban stream-water chemistry variability. *Biogeochemistry*, *144*(1), 61–84. https://doi.org/10.1007/s10533-019-00572-7

Bricker, O. P., Godfrey, A. E., & Cleaves, E. T. (1968). *Mineral-water interaction during the chemical weathering of silicates*. ACS Publications.

Bricker, S. B., Longstaff, B., Dennison, W., Jones, A., Boicourt, K., Wicks, C., & Woerner, J. (2008). Effects of nutrient enrichment in the nation's estuaries: A decade of change. *Harmful Algae*, *8*(1), 21–32. https://doi.org/10.1016/j.hal.2008.08.028

Burke, A., Present, T. M., Paris, G., Rae, E. C., Sandilands, B. H., Gaillardet, J., et al. (2018). Sulfur isotopes in rivers: Insights into global weathering budgets, pyrite oxidation, and the modern sulfur cycle. *Earth and Planetary Science Letters*, *496*, 168–177. https://doi.org/10.1016/j.epsl.2018.05.022

Burt, E. I., Bill, M., Conrad, M. E., Quispe, A. J. C., Christensen, J. N., Hilton, R. G., et al. (2021). Conservative transport of dissolved sulfate across the Rio Madre de Dios floodplain in Peru. *Geology*, *49*(9), 1064–1068. https://doi.org/10.1130/g48997.1

Buttle, J. M. (1994). Isotope hydrograph separations and rapid delivery of pre-event water from drainage basins. *Progress in Physical Geography*, *18*(1), 16–41. https://doi.org/10.1177/030913339401800102

Cai, M., Johnson, A. M., Schwartz, J. S., Moore, S. E., & Kulp, M. A. (2011). Response of soil water chemistry to simulated changes in acid deposition in the great smoky mountains. *Journal of Environmental Engineering*, *137*(7), 617–628. https://doi.org/10.1061/(asce)ee.1943-7870.0000354

Calmels, D., Gaillardet, J., Brenot, A., & France-Lanord, C. (2007). Sustained sulfide oxidation by physical erosion processes in the Mackenzie River basin: Climatic perspectives. *Geology*, *35*(11), 1003–1006. https://doi.org/10.1130/g24132a.1

Canfield, D. E., Raiswell, R., Westrich, J. T., Reaves, C. M., & Berner, R. A. (1986). The use of chromium reduction in the analysis of reduced inorganic sulfur in sediments and shales. *Chemical Geology*, *54*(1–2), 149–155. https://doi.org/10.1016/0009-2541(86)90078-1

Canfield, D. E., Stewart, F. J., Thamdrup, B., De Brabandere, L., Dalsgaard, T., Delong, E. F., & Ulloa, O. (2010). A cryptic sulfur cycle in oxygen-minimum–zone waters off the Chilean coast. *Science*, *330*(6009), 1375–1378. https://doi.org/10.1126/science.1196889

Caraco, N. F. (1993). Disturbance of the phosphorus cycle: A case of indirect effects of human activity. *Trends in Ecology & Evolution*, *8*(2), 51–54. https://doi.org/10.1016/0169-5347(93)90158-l

Caraco, N. F., Cole, J. J., & Likens, G. E. (1993). Sulfate control of phosphorus availability in lakes. *Hydrobiologia*, *253*(1), 275–280. https://doi.org/10.1007/bf00050748

Cardoso, R. B., Sierra-Alvarez, R., Rowlette, P., Flores, E. R., Gómez, J., & Field, J. A. (2006). Sulfide oxidation under chemolithoautotrophic denitrifying conditions. *Biotechnology and Bioengineering*, *95*(6), 1148–1157. https://doi.org/10.1002/bit.21084

Castiblanco, E. S., Groffman, P. M., Duncan, J., Band, L. E., Doheny, E., Fisher, G. T., et al. (2023). Long-term trends in nitrate and chloride in streams in an exurban watershed. *Urban Ecosystems*, *26*(3), 831–844. https://doi.org/10.1007/s11252-023-01340-0

Charola, A. E., Pühringer, J., & Steiger, M. (2007). Gypsum: A review of its role in the deterioration of building materials. *Environmental Geology*, *52*(2), 339–352. https://doi.org/10.1007/s00254-006-0566-9

Chesapeake Bay Program Office (CBPO). (2022). *One-meter resolution land cover Dataset for the Chesapeake Bay watershed, 2017/18*. University of Vermont Spatial Analysis Lab, Chesapeake Conservancy, and U.S. Geological Survey. Retrieved from http://www.chesapeakeconservancy.org

Christophersen, N., & Wright, R. F. (1981). Sulfate budget and a model for sulfate concentrations in stream water at Birkenes, a small forested catchment in southernmost Norway. *Water Resources Research*, *17*(2), 377–389. https://doi.org/10.1029/wr017i002p00377

Clair, J. S., Moon, S., Holbrook, W. S., Perron, J. T., Riebe, C. S., Martel, S. J., et al. (2015). Geophysical imaging reveals topographic stress control of bedrock weathering. *Science*, *350*(6260), 534–538. https://doi.org/10.1126/science.aab2210

Cleaves, E. T., Godfrey, A. E., & Bricker, O. P. (1970). Geochemical balance of a small catchment and its geomorphic implications. *Geological Society of America Bulletin*, *81*(10), 3015–3032. https://doi.org/10.1130/0016-7606(1970)81[3015:gboasw]2.0.co;2

Cook, F. J., Hicks, W., Gardner, E. A., Carlin, G. D., & Froggatt, D. W. (2000). Export of acidity in drainage water from acid sulphate soils. *Marine Pollution Bulletin*, *41*(7–12), 319–326. https://doi.org/10.1016/s0025-326x(00)00138-7

Cooney, K. S. (2005). A stable isotope investigation of precipitation nitrate.

Cosans, C. L., Gomes, M. L., Marsh, M. J., Moore, J., & Harman, C. J. (2024). Data associated with the publication: Similarities in sulfate isotopic signatures, storage, and transport across a suburban to forested land use gradient, despite large anthropogenic sulfate flux [Dataset]. Johns Hopkins Research Data Repository. https://doi.org/10.7281/T1/NU0VS7

Cosby, B. J., Hornberger, G. M., Wright, R. F., & Galloway, J. N. (1986). Modeling the effects of acid deposition: Control of long-term sulfate dynamics by soil sulfate adsorption. *Water Resources Research*, *22*(8), 1283–1291. https://doi.org/10.1029/wr022i008p01283

Cravotta, C. A. (1995). *Use of stable isotopes of carbon, nitrogen, and sulfur to identify sources of nitrogen in surface waters in the lower Susquehanna River basin, Pennsylvania*. US Geological Survey.

Crowley, W. P., Reinhardt, J., & Cleaves, E. T. (1975). *Geologic map of the Cockeysville quadrangle*. Maryland Geological Survey.

David, M. B., & Mitchell, M. J. (1987). Transformations of organic and inorganic sulfur: Importance to sulfate flux in an Adirondack forest soil. *JAPCA*, *37*(1), 39–44. https://doi.org/10.1080/08940630.1987.10466198

Davidson, C. I., Lindberg, S. E., Schmidt, J. A., Cartwright, L. G., & Landis, L. R. (1985). Dry deposition of sulfate onto surrogate surfaces. *Journal of Geophysical Research*, *90*(D1), 2123–2130. https://doi.org/10.1029/jd090id01p02123

Dean, W. E., Schreiber, B. C., Friedman, G. M., Hite, R. J., Nurmi, R. D., Raup, O. B., & Shearman, D. J. (1987). Trace and minor elements in evaporites. *Marine Evaporites*.

Dingman, S. L. (2015). *Physical hydrology* (pp. 586–593). Waveland press.

Duncan, J. M., Welty, C., Kemper, J. T., Groffman, P. M., & Band, L. E. (2017). Dynamics of nitrate concentration-discharge patterns in an urban watershed. *Water Resources Research*, *53*(8), 7349–7365. https://doi.org/10.1002/2017wr020500

Eckhardt, K. (2005). How to construct recursive digital filters for baseflow separation. *Hydrological Processes: International Journal*, *19*(2), 507–515. https://doi.org/10.1002/hyp.5675

Eng, L. E., & Scanlon, T. M. (2021). Comparison of northeastern and southeastern US catchment response to the declines in atmospheric sulfur deposition. *Atmospheric Environment*, *253*, 118365. https://doi.org/10.1016/j.atmosenv.2021.118365

Evans, H. E., Dillon, P. J., & Molot, L. A. (1997). The use of mass balance investigations in the study of the biogeochemical cycle of sulfur. *Hydrological Processes*, *11*(7), 765–782. https://doi.org/10.1002/(sici)1099-1085(199706)11:7<765::aid-hyp520>3.0.co;2-f

Farquhar, J., Canfield, D. E., Masterson, A., Bao, H., & Johnston, D. (2008). Sulfur and oxygen isotope study of sulfate reduction in experiments with natural populations from Faellestrand, Denmark. *Geochimica et Cosmochimica Acta*, *72*(12), 2805–2821. https://doi.org/10.1016/j.gca.2008.03.013

Fertilizer Use Act. (2011). Retrieved from https://mde.maryland.gov/programs/water/TMDL/TMDLImplementation/Documents/Archive/Regional_Meetings/Fall2013/presentations/Fertilizer_Use_Act_110513.pdf

Fraser, J. C., Bazuin, J. T., Band, L. E., & Grove, J. M. (2013). Covenants, cohesion, and community: The effects of neighborhood governance on lawn fertilization. *Landscape and Urban Planning*, *115*, 30–38. https://doi.org/10.1016/j.landurbplan.2013.02.013

Fritz, P., Basharmal, G. M., Drimmie, R. J., Ibsen, J., & Qureshi, R. M. (1989). Oxygen isotope exchange between sulphate and water during bacterial reduction of sulphate. *Chemical Geology: Isotope Geoscience section*, *79*(2), 99–105. https://doi.org/10.1016/0168-9622(89)90012-2

Gayle, G. A., Reddy, G. B., Reddy, M. R., Ross, S. M., & Dunn, S. J. (1981). *Factors to be considered in disposing domestic waste on problem sites and appraisal of water quality in a piedmont setting*. Water Resources Research Institute of the University of North Carolina.

Gislason, S. R., & Torssander, P. (2006). Response of sulfate concentration and isotope composition in Icelandic rivers to the decline in global atmospheric SO_2 emissions into the North Atlantic region. *Environmental Science & Technology*, *40*(3), 680–686. https://doi.org/10.1021/es051325o

Groffman, P. M., Law, N. L., Belt, K. T., Band, L. E., & Fisher, G. T. (2004). Nitrogen fluxes and retention in urban watershed ecosystems. *Ecosystems*, *7*(4), 393–403. https://doi.org/10.1007/s10021-003-0039-x

Hao, T., Xiang, P., Mackey, H. R., Chi, K., Lu, H., Chui, H., et al. (2014). A review of biological sulfate conversions in wastewater treatment. *Water Research*, *65*, 1–21. https://doi.org/10.1016/j.watres.2014.06.043

Hill, F. B. (1969). *Ivy Hill, Oregon Ridge Key, bought for unnamed party*. The Baltimore Sun.

Hinckley, E. S., Crawford, J. T., Fakhraei, H., & Driscoll, C. T. (2020). A shift in sulfur-cycle manipulation from atmospheric emissions to agricultural additions. *Nature Geoscience*, *13*(9), 597–604. https://doi.org/10.1038/s41561-020-0620-3

Hintz, W. D., & Relyea, R. A. (2019). A review of the species, community, and ecosystem impacts of road salt salinisation in fresh waters. *Freshwater Biology*, *64*(6), 1081–1097. https://doi.org/10.1111/fwb.13286

Huang, J., Yuro, R., & Romeo, G. A., Jr. (1995). Photooxidation of corbett fractions of asphalt. *Fuel Science and Technology International*, *13*(9), 1121–1134. https://doi.org/10.1080/08843759508947727

Humphrey, C. P., Jernigan, J., Iverson, G., Serozi, B., O'Driscoll, M., Pradhan, S., & Bean, E. (2016). Field evaluation of nitrogen treatment by conventional and single-pass sand filter onsite wastewater systems in the North Carolina piedmont. *Water, Air, & Soil Pollution*, *227*(8), 1–17. https://doi.org/10.1007/s11270-016-2958-0

Iverson, G., Humphrey, C. P., Jr., O'Driscoll, M. A., Sanderford, C., Jernigan, J., & Serozi, B. (2018). Nutrient exports from catchments with varying septic system densities in the North Carolina piedmont. *Journal of Environmental Management*, *211*, 206–217. https://doi.org/10.1016/j.jenvman.2018.01.063

Jacques, D., Wang, L., Martens, E., & Mallants, D. (2010). Modelling chemical degradation of concrete during leaching with rain and soil water types. *Cement and Concrete Research*, *40*(8), 1306–1313. https://doi.org/10.1016/j.cemconres.2010.02.008

Johnson, N. M., Driscoll, C. T., Eaton, J. S., Likens, G. E., & McDowell, W. H. (1981). 'Acid rain', dissolved aluminum and chemical weathering at the Hubbard Brook experimental forest, New Hampshire. *Geochimica et Cosmochimica Acta*, *45*(9), 1421–1437. https://doi.org/10.1016/0016-7037(81)90276-3

Johnston, D. T., Gill, B. C., Masterson, A., Beirne, E., Casciotti, K. L., Knapp, A. N., & Berelson, W. (2014). Placing an upper limit on cryptic marine sulphur cycling. *Nature*, *513*(7519), 530–533. https://doi.org/10.1038/nature13698

Kaplan, I. R., & Rittenberg, S. C. (1964). Microbiological fractionation of sulphur isotopes. *Microbiology*, *34*(2), 195–212. https://doi.org/10.1099/00221287-34-2-195

Kaushal, S. S., & Belt, K. T. (2012). The urban catchment continuum: Evolving spatial and temporal dimensions. *Urban Ecosystems*, *15*(2), 409–435. https://doi.org/10.1007/s11252-012-0226-7

Kaushal, S. S., Duan, S., Doody, T. R., Haq, S., Smith, R. M., Johnson, T. A. N., et al. (2017). Human-accelerated weathering increases salinization, major ions, and alkalinization in fresh water across land use. *Applied Geochemistry*, *83*, 121–135. https://doi.org/10.1016/j.apgeochem.2017.02.006

Kester, C. L., Baron, J. S., & Turk, J. T. (2003). Isotopic study of sulfate sources and residence times in a subalpine catchment. *Environmental Geology*, *43*(5), 606–613. https://doi.org/10.1007/s00254-002-0684-y

Ketterings, Q., Miyamoto, C., Mathur, R. R., Dietzel, K., & Gami, S. (2011). A comparison of soil sulfur extraction methods. *Soil Science Society of America Journal*, *75*(4), 1578–1583. https://doi.org/10.2136/sssaj2010.0407

Krouse, H. R., & Mayer, B. (2000). Sulphur and oxygen isotopes in sulphate. In *Environmental tracers in subsurface hydrology* (pp. 195–231). Springer.

Lamers, L. P., Tomassen, H. B., & Roelofs, J. G. (1998). Sulfate-induced eutrophication and phytotoxicity in freshwater wetlands. *Environmental Science & Technology*, *32*(2), 199–205. https://doi.org/10.1021/es970362f

Lawrence, G. B. (2002). Persistent episodic acidification of streams linked to acid rain effects on soil. *Atmospheric Environment*, *36*(10), 1589–1598. https://doi.org/10.1016/s1352-2310(02)00081-x

Lewis, G. P., Mitchell, J. D., Andersen, C. B., Haney, D. C., Liao, M., & Sargent, K. A. (2007). Urban influences on stream chemistry and biology in the big brushy creek catchment, South Carolina. *Water, Air, and Soil Pollution*, *182*(1), 303–323. https://doi.org/10.1007/s11270-007-9340-1

Likens, G. E., & Bormann, F. H. (1974). Acid rain: A serious regional environmental problem. *Science*, *184*(4142), 1176–1179. https://doi.org/10.1126/science.184.4142.1176

Lindberg, S. E., Lovett, G. M., Richter, D. D., & Johnson, D. W. (1986). Atmospheric deposition and canopy interactions of major ions in a forest. *Science*, *231*(4734), 141–145. https://doi.org/10.1126/science.231.4734.141

Lloyd, R. M. (1968). Oxygen isotope behavior in the sulfate–water system. *Journal of Geophysical Research*, *73*(18), 6099–6110. https://doi.org/10.1029/jb073i018p06099

Magee, E. A., Richardson, C. J., Hughes, R., & Cummings, J. H. (2000). Contribution of dietary protein to sulfide production in the large intestine: An in vitro and a controlled feeding study in humans. *The American Journal of Clinical Nutrition*, *72*(6), 1488–1494. https://doi.org/10.1093/ajcn/72.6.1488

Mayer, B., Fritz, P., Prietzel, J., & Krouse, H. R. (1995). The use of stable sulfur and oxygen isotope ratios for interpreting the mobility of sulfate in aerobic forest soils. *Applied Geochemistry*, *10*(2), 161–173. https://doi.org/10.1016/0883-2927(94)00054-a

McAvoy, D. C., Decarvalho, A. J., Nielsen, A. M., & Cano, M. L. (2009). Investigation of an onsite wastewater treatment system in sandy soil: Modeling the fate of surfactants. *Environmental Toxicology and Chemistry: International Journal*, *21*(12), 2623–2630. https://doi.org/10.1002/etc.5620211214

McMahon, P., Beauchamp, V. B., Casey, R. E., Salice, C. J., Bucher, K., Marsh, M., & Moore, J. (2021). Effects of stream restoration by legacy sediment removal and floodplain reconnection on water quality. *Environmental Research Letters*, *16*(3), 035009. https://doi.org/10.1088/1748-9326/abe007

Mizutani, Y., & Rafter, T. A. (1969). *Oxygen isotopic composition of sulphates. Part 4. Bacterial fractionation of oxygen isotopes in the reduction of sulphate and in the oxidation of sulphur*. Inst. of Nuclear Sciences.

Moore, J., Bird, D. L., Dobbis, S. K., & Woodward, G. (2017). Nonpoint source contributions drive elevated major ion and dissolved inorganic carbon concentrations in urban catchments. *Environmental Science and Technology Letters*, *4*(6), 198–204. https://doi.org/10.1021/acs.estlett.7b00096

Nehlich, O. (2015). The application of sulphur isotope analyses in archaeological research: A review. *Earth-Science Reviews*, *142*, 1–17. https://doi.org/10.1016/j.earscirev.2014.12.002

Nehls, T., Rokia, S., Mekiffer, B., Schwartz, C., & Wessolek, G. (2013). Contribution of bricks to urban soil properties. *Journal of Soils and Sediments*, *13*(3), 575–584. https://doi.org/10.1007/s11368-012-0559-0

Nielsen, A. M., Decarvalho, A. J., McAvoy, D. C., Kravetz, L., Cano, M. L., & Anderson, D. L. (2009). Investigation of an onsite wastewater treatment system in sandy soil: Site characterization and fate of anionic and nonionic surfactants. *Environmental Toxicology and Chemistry: International Journal*, *21*(12), 2606–2616. https://doi.org/10.1002/etc.5620211212

Patel, K. F., Fernandez, I. J., Nelson, S. J., Malcomb, J., & Norton, S. A. (2020). Contrasting stream nitrate and sulfate response to recovery from experimental catchment acidification. *Biogeochemistry*, *151*(2), 127–138. https://doi.org/10.1007/s10533-020-00711-5

Pellerin, A., Antler, G., Holm, S. A., Findlay, A. J., Crockford, P. W., Turchyn, A. V., et al. (2019). Large sulfur isotope fractionation by bacterial sulfide oxidation. *Science Advances*, *5*(7), eaaw1480. https://doi.org/10.1126/sciadv.aaw1480

Pester, M., Knorr, K., Friedrich, M. W., Wagner, M., & Loy, A. (2012). Sulfate-reducing microorganisms in wetlands–fameless actors in carbon cycling and climate change. *Frontiers in Microbiology*, *3*, 72. https://doi.org/10.3389/fmicb.2012.00072

Pinder, G. F., & Jones, J. F. (1969). Determination of the ground-water component of peak discharge from the chemistry of total runoff. *Water Resources Research*, *5*(2), 438–445. https://doi.org/10.1029/wr005i002p00438

Price, J. R., & Szymanski, D. W. (2014). The effects of road salt on stream water chemistry in two small forested catchments, Catoctin mountain, Maryland, USA. *Aquatic Geochemistry*, *20*(2), 243–265. https://doi.org/10.1007/s10498-013-9193-8

Putnam, S. M. (2018). *The influence of landscape structure on storage and streamflow generation in a Piedmont catchment*. Doctoral dissertation. Johns Hopkins University.

Rajan, S. (1978). Sulfate adsorbed on hydrous alumina, ligands displaced, and changes in surface charge. *Soil Science Society of America Journal*, *42*(1), 39–44. https://doi.org/10.2136/sssaj1978.03615995004200010009x

Reverey, F., Grossart, H., Premke, K., & Lischeid, G. (2016). Carbon and nutrient cycling in kettle hole sediments depending on hydrological dynamics: A review. *Hydrobiologia*, *775*(1), 1–20. https://doi.org/10.1007/s10750-016-2715-9

Rice, K. C., Scanlon, T. M., Lynch, J. A., & Cosby, B. J. (2014). Decreased atmospheric sulfur deposition across the southeastern US: When will catchments release stored sulfate? *Environmental Science & Technology*, *48*(17), 10071–10078. https://doi.org/10.1021/es501579s

Riscassi, A., Scanlon, T., & Galloway, J. (2019). Stream geochemical response to reductions in acid deposition in headwater streams: Chronic versus episodic acidification recovery. *Hydrological Processes*, *33*(4), 512–526. https://doi.org/10.1002/hyp.13349

Roden, E. E., & Edmonds, J. W. (1997). Phosphate mobilization in iron-rich anaerobic sediments: Microbial Fe (III) oxide reduction versus iron-sulfide formation. *Archiv für Hydrobiologie*, *139*(3), 347–378. https://doi.org/10.1127/archiv-hydrobiol/139/1997/347

Selim, H. M., Gobran, G. R., Guan, X., & Clarke, N. (2004). Mobility of sulfate in forest soils: Kinetic modeling. *Journal of Environmental Quality*, *33*(2), 488–495. https://doi.org/10.2134/jeq2004.4880

Shanley, J. B., Mayer, B., Mitchell, M. J., Michel, R. L., Bailey, S. W., & Kendall, C. (2005). Tracing sources of streamwater sulfate during snowmelt using S and O isotope ratios of sulfate and 35 S activity. *Biogeochemistry*, *76*(1), 161–185. https://doi.org/10.1007/s10533-005-2856-9

Shimp, R. J., Lapsins, E. V., & Ventullo, R. M. (1994). Chemical fate and transport in a domestic septic system: Biodegradation of linear alkylbenzene sulfonate (LAS) and nitrilotriacetic acid (NTA). *Environmental Toxicology and Chemistry: International Journal*, *13*(2), 205–212. https://doi.org/10.1002/etc.5620130204

Shober, A. L., Wiese, C., & Denny, G. C. (2011). Soil pH and the home landscape or garden. *Edis*, *2011*(5/6). https://doi.org/10.32473/edis-ss480-2011

Sim, M. S., Bosak, T., & Ono, S. (2011). Large sulfur isotope fractionation does not require disproportionation. *Science*, *333*(6038), 74–77. https://doi.org/10.1126/science.1205103

Strachan, N., Davis, L., Donnelly, R., Fath, B., Martin, K., Moore, T., et al. (2009). *Road salt recommendations to the Baltimore county council. Road salt working group* (Vol. 42). Baltimore County Advisory Commission on Environmental Quality.

Taboada-Castro, M. M., Rodríguez-Blanco, M. L., Diéguez, A., Palleiro, L., Oropeza-Mota, J. L., & Taboada-Castro, M. T. (2015). Effects of changing land use from agriculture to forest on stream water quality in a small basin in NW Spain. *Communications in Soil Science and Plant Analysis*, *46*(sup1), 353–361. https://doi.org/10.1080/00103624.2014.989109

Torres, M. A., West, A. J., Clark, K. E., Paris, G., Bouchez, J., Ponton, C., et al. (2016). The acid and alkalinity budgets of weathering in the Andes– Amazon system: Insights into the erosional control of global biogeochemical cycles. *Earth and Planetary Science Letters*, *45*, 381–391. https://doi.org/10.1016/j.epsl.2016.06.012

Tuttle, J. H., Dugan, P. R., & Randles, C. I. (1969). Microbial sulfate reduction and its potential utility as an acid mine water pollution abatement procedure. *Applied Microbiology*, *17*(2), 297–302. https://doi.org/10.1128/am.17.2.297-302.1969

USEPA. (2002). Onsite wastewater treatment systems manual.

U.S. Geological Survey. (2016). National water information system data available on the world wide web (USGS water data for the nation). Retrieved from http://waterdata.usgs.gov/nwis/

U.S. Geological Survey. (2017). National hydrography Dataset Plus high resolution (NHDPlus HR) - USGS national map downloadable data collection.

Van Stempvoort, D. R., Reardon, E. J., & Fritz, P. (1990). Fractionation of sulfur and oxygen isotopes in sulfate by soil sorption. *Geochimica et Cosmochimica Acta*, *54*(10), 2817–2826. https://doi.org/10.1016/0016-7037(90)90016-e

Welty, C., Moore, J., Bain, D. J., Talebpour, M., Kemper, J. T., Groffman, P. M., & Duncan, J. M. (2023). Spatial heterogeneity and temporal stability of baseflow stream chemistry in an urban watershed. *Water Resources Research*, *59*(1), e2021WR031804. https://doi.org/10.1029/2021wr031804

Wilhelm, S. R., Schiff, S. L., & Cherry, J. A. (1994). Biogeochemical evolution of domestic waste water in septic systems: 1. Conceptual model. *Groundwater*, *32*(6), 905–916. https://doi.org/10.1111/j.1745-6584.1994.tb00930.x

Wilhelm, S. R., Schiff, S. L., & Robertson, W. D. (1994). Chemical fate and transport in a domestic septic system: Unsaturated and saturated zone geochemistry. *Environmental Toxicology and Chemistry: International Journal*, *13*(2), 193–203. https://doi.org/10.1002/etc.5620130203

Wolman, M. G. (1987). Sediment movement and knickpoint behavior in a small piedmont drainage basin. *Geografiska Annaler - Series A: Physical Geography*, *69*(1), 5–14. https://doi.org/10.1080/04353676.1987.11880192

Zak, I., Sakai, H., & Kaplan, I. R. (1980). Factors controlling $^{18}O/^{16}O$ and $^{34}S/^{32}S$ isotope rations of ocean sulfates, evaporites, and interstitial sulfates from modern deep sea sediments. In Y. Horibe & K. Sakurashi (Eds.), *Isotope marine chemistry* (pp. 339–376).

Zhu, J., He, Y., Zhu, Y., Huang, M., & Zhang, Y. (2018). Biogeochemical sulfur cycling coupling with dissimilatory nitrate reduction processes in freshwater sediments. *Environmental Reviews*, *26*(2), 121–132. https://doi.org/10.1139/er-2017-0047

References From the Supporting Information

Daddow, R. L. (1983). *Growth-limiting soil bulk densities as influenced by soil texture*. Watershed Systems Development Group, USDA Forest Service.